UNIVERSIDAD NACIONAL AUTÓNOMA DE MÉXICO

FACULTAD DE INGENIERÍA

Análisis Dinámico de la Muerte Celular:

Apoptosis

Sysytems Analysis and Dynamics of Cellular Self-Destruction Systems: Apoptosis

T E S I S

QUE PARA OBTENER EL TÍTULO DE:

Maestro en Ingeniería

PRESENTA:

Fernando López Caamal

DIRECTOR DE TESIS:

Dr Jaime Alberto Moreno Pérez

Dr Dimitrios Kalamatianos

· 2009 ·

Jurado Asignado

Presidente : Dr. Alvarez Icaza Longorá Luis Agustín

Secretario : Dr. Alvarez Calderón Jesús

Vocal : Dr. Moreno Pérez Jaime Alberto

1^{er} Suplente: Dr. Bullinger Eric

2^{do} Suplente: Dr. Kalamatianos Dimitrios

Lugar donde se realializó la tesis:

- Facultad de Ingeniería, UNAM
- Instituto Hamilton, NUIM

TUTOR DE LA TESIS

Dr. Moreno Pérez Jaime Alberto

FIRMA

Acronyms and notation

EXAP	Extrinsic Apoptosis Pathway
INAP	Intrinsic Apoptosis Patway
CARP	Cellular Apoptosis Regulatory Protein
IAP	Inhibitor of Apoptosis Protein
SSV (μ^{-1})	Structural Singular Value
LFT	Linear Fractional Transformation
$[X]$	Concentration of X
$[E:S]$	Concentration of E binded to S

Contents

List of Figures

List of Tables

Abstract

In recent years, the need for a better understanding and more specific applications in Biology, has lead to a synergy between theoretical and experimental Biology and Systems Theory. This relatively new application field is called Systems Biology. In a clinical context, this fusion intends to provide a systematic guideline for unveiling the core mechanisms of several diseases. In the present work, the dynamical study of the mathematical model of the Extrinsic and Intrinsic Apoptosis Pathways is performed in order to provide a better characterization of the pathways. It is important to remark that malfunction of this cellular process has been involved with neurodegenerative diseases and cancer.

In order to identify the most important reactions in the pathway and to determine the role of each one, a descentralized controller scheme is identified and analyzed in both pathways and a bifurcation analysis is performed to the Extrinsic Apoptosis Pathway and finally the robustness of the stability and performance in the linearization of both pathways is studied.

Chapter 1

Introduction

In this section the concepts of Systems Biology and cell death processes are introduced. In Chapter 2, the dynamical models which reproduce the reactions dynamics in two different apoptosis pathways are presented. Chapter 3 shows the steady state analysis and decentralized structure of the systems. Then, in Chapter 4 the qualitative behavior of the system is explained via a bifurcation diagram and, finally, the robustness of the stability and performance indexes are analyzed in Chapter 5.

1.1 Systems biology concept

The idea of understanding the phenomena present in a living being is not new. In the late 1940's, Norbert Wiener in his book *Cybernetics* proposed the motifs present in the living beings as a benchmark for human-made designs. Although in this approach some mechanisms present in the living beings are studied and understood, the main goal is to apply this knowledge to the human-made designs rather than provide a holistic understanding of the living being. In 1944, Schrödinger posed the question: Can the phenomena present in the living matter be explained with the current physical knowledge? Or are they explained with a new physical law? (Schrödinger, 1944). Certainly, the hypotheses posed in order to answer the previous questions involved yet undeveloped experimental work. Recent technological developments have provided a means for testing some of these hypotheses and to obtain meaningful answers. However the technical availability of experimental equipment and the expertise in its use, is just one part for getting information of process occurring in a cell, for example. A sound biochemical knowledge of the phenomenon itself and a systematic way for testing the hypotheses have to be available, i.e., the biological knowledge can claim how the mechanism of a certain phenomenon happens and a systematic approach provides the guideline for accepting or refusing this claim. With the identification of the structure of DNA by Watson and Crick (Watson and Crick, 1953), the basis for understanding a cellular process as a well defined mechanism was set in motion. Since then, the development in both the experimental and theoretical Molecular Biology has furthered the understanding. As years went by, a wide variety of processes, ranging from

the cellular division to the evolution of viruses, have been studied.

A further step is to abstract this biological knowledge into a set of dynamical and algebraic equations. In the remaining of this thesis, the term 'model' will refer to this set of equations. After this model has been experimentally validated, it can be used to explore cell behavior in computational experiments (in silico analysis) and further analytical studies can be performed to infer some dynamical properties. This last step is main the theme of this thesis.

The disciplines of Biology and Systems Theory can lead to a better biological understanding of cellular dynamics. In turn Systems Theory finds new challenges which will lead to a further development of the theory. Some examples of the collaboration of these areas can be found in the terms Computational Physiology and Systems Biology. This later term was first used by Kitano, who states: "*Systems biology is a new field of Biology that aims to develop a system-level understanding of biological systems. System level understanding requires a set of principles and methodologies that links the behaviors of molecules to system characteristics and functions. Ultimately, cells, organisms, and human beings will be described and understood at the system level grounded on a consistent framework of knowledge that is underpinned by the basic principles of physics*" (Kitano, 2001).

In contrast to Kitano, other authors define it as a synergy of different disciplines rather than a pure Biological area. "*[...]Systems biology is the coordinated study of biological systems by (1) investigating the components of cellular networks and their interactions, (2) applying experimental high-throughput and whole-genome techniques, and (3) integrating computational methods with experimental efforts. [...] Systems biology comprises experimentation and computational modeling. To this end, it integrates approaches from diverse areas of science such as biology, chemistry, physics, mathematics, applied science, engineering, cybernetics, and computer science. By demanding new strategies, it also stimulates their further development and contributes to new solutions.[...]*" (Klipp et al., 2005)

Recently, the methods of Control Engineering have been used to provide this systematic insight, for providing a better understanding of a certain biological processes. In (Wellstead et al., 2008) and (Sontag, 2005) a statement of Biological problems and the potential of applying a Systems Theory approach to them are presented in Engineering terms.

1.2 Cell death signalling

In general, cell death is a process as important as the cell division itself, since its fundamental aim is to keep tissue healthy and functioning correctly via the removal of old, damaged or unhealthy cells. This is a well studied phenomenon which has attracted the attention of researchers from different fields. In the last decade, the study of the mechanism in which a cell dies has been divided into three categories (Lockshin and Zakeri, 2004): autophagy, apoptosis and necrosis.

- Autophagy
  The term autophagy is derived from Greek roots: *auto*, meaning 'self', and

phagy, 'to eat'. It is a well-known physiological process involved in routine turnover of cells constituents. In this process a specific membrane in the cytosol engulfs the organelle to be removed and it is digested by lysosomal enzymes. Figure 1.1 shows the relationship of this type of cell death with the outcome of a cell: although autophagy mostly allows cells to adapt to stress, massive autophagy can also lead to cell death. This Figure also shows the existence of a competitive scheme between this process of adaptation and a well known cell death process called apoptosis.

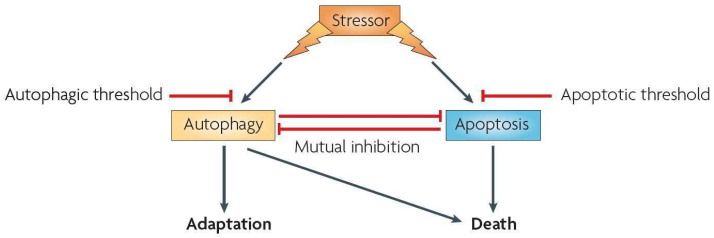

Figure 1.1: Qualitative interaction among autophagy and apoptosis (Image taken from Lockshin and Zakeri 2004)

- Apoptosis
  The term apoptosis has also Greek roots: *apo* which means 'off' and *ptosis*, 'falling', thus apoptosis resembles leaves falling of a tree. It is a programmed cell death based on the activation of caspases. The Caspases (Cysteine-ASPartic Acid proteaASES) are a family of proteolytic acids which cleaves after asparte residues in substrate proteins. There exist two type of caspases:

  - Initiator caspases
    They are caspases activated in response to a specific triggering event.
    - Caspase 8: is activated via the death-receptor ligands in the outer membrane of the cell.
    - Caspase 9: is active when bounded to a special protein called Apoptosome.
    - Caspase 2: is activated when DNA damage has been encountered.
  - Effector caspases
    They are activated via the initiator caspases. This subtype of caspases include the Caspases 3, 6 and 7.

  In the case of apoptosis, Caspase 3 is the caspase that exerts the most representative effect in the cell dismantling. It can be activated by either Caspase 8 or Caspase 9, the extrinsic or intrinsic apoptosis pathway. The activation of caspases is present in a wide variety of processes: from virus propagation (Wurzer et al., 2003) to blood clotting and wound healing (Rai et al., 2005) and, as stated above, the core mechanism of apoptosis.

When the apoptosis mechanism is not triggered correctly, the natural cell cycle is disrupted. When apoptosis is underactivated the survival of cancer cells can be promoted. On the other hand, the over activation of the mechanism can kill healthy cells: in the nervous system the death of a kind of cells has been implicated in Parkinson's disease.

In recent years, the developments in the optoelectronic industry have made available powerful automated microscopes which can give meaningful information to the experimental biologists. In the cellular level, imaging via ionized dyes is the *ad hoc* media for recovering qualitative data from a wet experiment. See (Paul et al., 2008), for example.

- Necrosis
  This term includes all the phenomena not included in the above foregoing concepts (Lockshin and Zakeri, 2004). Since it can be caused by a wide variety of reasons, the actual classification is not straightforward and lies beyond the scope of this informal introduction.

1.3 Outline of the thesis

This thesis is focused on the study of the dynamics of two apoptosis pathways: the Extrinsic Apoptosis Pathway (EXAP) (Eissing, 2007) and the Intrinsic Apoptosis Pathway (INAP) (Rehm et al., 2006). The main aim of this study is to provide a better insight in the pathway and to classify the reactions according to their relevance in the structural bistability and sensitivity of the local stability and local performance. Given the complexity of the networks, no dynamical properties could be obtained and just a numerical characterization was carried out. In previous works (Eissing, 2007) and (Carotenuto et al., 2007) a Monte Carlo analysis and a one and two parameter bifurcation analysis are performed in order to identify the set of parameters that lead to a bistable scenario, respectively. In this work, a one parameter bifurcation analysis is performed in order to determine the possible behaviors of the network and the feasibility to reach them.

In the next Chapter, the dynamical models which reproduce the reaction dynamics in the two different apoptosis pathways are presented. In Chapter 3 a methodology for identifying the structure of the model is presented and a steady state analysis is performed, which characterizes the bistable behavior of the model of the EXAP. In Chapter 4 the characterization of the bistable property of the EXAP model is presented. Finally in Chapter 5, robust stability and performance indexes are computed for both apoptosis pathways. To conclude this Chapter, a list of the main contributions is presented.

1.4 Main contributions

- A proportional derivative control mechanism is identified arising from a particular reaction diagram

- A bifurcation analysis is performed for the Extrinsic Apoptosis Pathway model, identifying some of the possible behaviors of the network. In this regard, a robustness index is evaluated in terms of the impact of the variation of one parameter in the structural bistability property of the network
- The sensitivity of the models analyzed is performed via the Structural Singular Value

Chapter 2

Apoptosis models

This Chapter presents an overview of two Apoptosis Pathways as deterministic dynamical systems. Both models are build upon the knowledge of the interaction among the reactants present in each pathway. Both, the INAP and EXAP model, reproduce accurately the concentration of the compounds involved in each mechanism. Remarkably, the model of the EXAP has the interesting dynamical property of bistability.

2.1 Introduction

Once identified the chemical species interacting in a reaction network, a reaction diagram can be established (e.g. $\mathrm{A} + \mathrm{B} \longrightarrow \mathrm{C}$). From this reaction diagram, the assignation of a suitable reaction mechanism leads to a set of differential equations: the mathematical model of the reaction network. When a nominal set of parameters is selected for the model, quantitative analyses can be performed in order to determine the particular characteristics of the system: fixed points and stability, for instance. A more general analysis can be done in disregard of any numerical assignation to the parameters. The results of this later analysis are the properties of the reaction network, rather than the properties of a particular reaction. Consider for example the next reactions:

$$0 \underset{k_2}{\overset{k_1}{\rightleftharpoons}} \mathrm{A} \underset{k_4}{\overset{k_3}{\rightleftharpoons}} \mathrm{B}$$

The dynamical model with the election of mass action reaction mechanism (see Section 2.2.2) is:

$$\begin{aligned} [\dot{A}] &= k_1 - (k_2 + k_3)[A] + k_4[B] \\ [\dot{B}] &= k_3[A] - k_4[B] \end{aligned} \tag{2.1}$$

Its fixed point is:

$$([\bar{A}], [\bar{B}]) = \left(\frac{k_1}{k_2}, \frac{k_1 k_3}{k_2 k_4}\right)$$

As can be seen from the expression above the fixed point is unique for any definition of k_1, k_2, k_3, k_4. The stability analysis of the system (2.1) concludes that the fixed point will be stable if all the constants are positive. That is to say that the global stability is a property of the network. Nevertheless the location of a fixed point of interest is a characteristic of a specific system with specific constants.

The identification of the properties of a network can be in general very complicated. However, if it is achieved, a qualitative characterization of the behavior of the network can be inferred. In Chapter 3, the identification of the structure of the two apoptosis models are presented and a further steady state analysis is performed to find properties of the network.

The next subsection presents some basic definitions and an informal overview of the cell death mechanisms.

2.2 Fundamentals

In comparison to traditional engineering systems, biological systems present a wider variety of scales in both time and size in a single phenomenon. Moreover, the complexity of the biological systems make them cumbersome at a first glimpse and in particular cases difficult to analyze. Another important difference is that dynamic test and measurement are widely present in engineering design. However, the real-time data acquisition of a cellular process is, in general, a technical challenge.

Despite these difficulties, the principle of biological phenomena can be explained on a chemical basis. Some of these concepts are introduced in the following subsections. First a protein degradation mechanism, then two reactions mechanism and finally general models for reaction networks will be presented.

2.2.1 Protein degradation

Most of the proteins that are degraded within the cell (in the cytosol) are delivered to large protein complexes called proteasomes, which are dispersed throughout the cell. Each proteasome consist of a central cylinder formed from multiple distinct proteases and acts on proteins that have been specifically marked for destruction by the attachment or a protein (ubiquitin) (Alberts et al., 2002). In general this is the mechanism in which a cleaved protein is degraded. In the case of apoptosis, this mechanism plays a very important role, since, once the pool of activated caspase has cleaved a protein, a final degradation has to be made to totally remove unwanted proteins.

It is important to remark that more ways of protein degradation have been identified, but for the scope of the present work the knowledge of the mechanism presented will be sufficient to make a plausible presentation of the topic.

2.2.2 Reaction Mechanisms

- Mass action Principle
  The Mass Action Principle states that the reaction rate is proportional to the probability of the reactant S_1 to meet S_2. In turn, this probability is proportional to

the concentration of the reactants to the power of the molecularity. Let R be a reaction from n reactants to m products:

$$\sum_{i=1}^{n} \mathrm{d_i S_i} \xrightarrow{v} \sum_{j=1}^{m} \mathrm{h_j P_j}$$

where d_i and h_j are the stoichiometric constants of the reactants S_i and the products P_j. Then the Mass action Principle states that :

$$\begin{aligned} v &\alpha \prod_{i=1}^{n} [S_i]^{d_i} \\ v &= k \prod_{i=1}^{n} [S_i]^{d_i} \end{aligned}$$

The proportionality constant k is defined by:

$$k(T) = \mathcal{A} e^{-\frac{E_a}{RT}}$$

where:

$\mathcal{A}$	Arrhenius constant	Reaction dependent
E_a	Activation Energy	Reaction dependent $[KJ]$
R	Universal Gas Constant	$8.314x10^{-3}[\frac{kJ}{molK}]$
T	Absolute temperature	$[K]$

In the rest of this work, the dependence of k on the temperature will be considered to be negligible.

In general, the velocity v of reaction is the rate of "vanishing" of the reactants S_i and of "creation" of the products P_j. Stated in mathematical terms,

$$\begin{aligned} \frac{d}{dt} S_i &= -v \\ \frac{d}{dt} P_j &= v \end{aligned}$$

- Catalyzed Reactions
  Catalyzed reactions are performed in several steps and in the presence of a catalyzing agent, whose role is to modify the activation energy of the reaction. The basic scheme of this type or reactions is:

$$\mathrm{S} + \mathrm{E} \underset{k_-}{\overset{k_+}{\rightleftharpoons}} \mathrm{E{:}\,S} \xrightarrow{k_p} \mathrm{P} + \mathrm{E}$$

where E stands for the enzyme, S for the substrate, E:S is the complex enzyme-substrate and P, the product. Under the assumption that the total amount of

enzyme (E:S + E) remains constant in time, the velocity of reaction from the substrate to the product yields:

$$-r_s = \frac{k_+ k_p [E][S]}{k_+[S] + k_- + k_p}$$

Normally, this equation is referred to as the Michaelis-Menten equation.

Catalyzed reactions exhibit a wide variety of behaviors depending on the details of the mechanism involved, for instance, it can either accelerate or slowdown the rate in which the product is being formed (Klipp et al., 2005).

2.2.3 Model of a reaction network

In general, the set of differential equations that arise from a reaction network is nonlinear and hence can exhibit a wide range of behaviors, such as multistability or oscillatory responses for certain ranges of the parameters.

In general, let this nonlinear system be described by

$$\frac{d}{dt}\mathbf{S} \quad = \quad \mathbf{f}(\mathbf{S}(t), \mathbf{p}) \qquad \mathbf{S}(0) = \mathbf{S}_0$$

where $\mathbf{S}$ is a vector containing the concentrations of all the species involved and $\mathbf{p}$ is a vector of parameters.

Due to the structure of a reaction network, the foregoing differential equation has a well defined structure defined by the reaction diagram. The information contained in this diagram can be synthesized the linear map $g : v \in Re \longrightarrow \frac{d}{dt}S$:

$$\frac{d}{dt}S \quad = \quad \mathbf{N}(\mathbf{p})v(\mathbf{S})$$

where $\mathbf{N}$ is a matrix whose $ij-th$ element is the stoichiometrical coefficient of the $i-th$ compound in the $j-th$ reaction. As a convention the sign of this element is positive if the compound is a product and negative if it is a substrate. This matrix is usually referred to as the stoichiometric matrix. v stands for the velocity rate of each reaction. Note that the fact that the concentrations are non-negative, cannot be considered in this approach.

The information contained in the stoichiometric matrix is the linear combination of reactions that, although they have a non-zero value, the product $\mathbf{N}v_*$ equals zero -if $v_* \in ker(N)$- and lead to a stationary state in the concentration of the reactants.

Also in this approach, a further reduction of the model can be achieved provided the matrix $\mathbf{N}$ is not full rank, since some of the concentrations will be just a linear combination of the linear independent ones.

Another modeling approach is presented in (Feinberg, 1979). In these notes, the term 'specie' is used to refer to every chemical compound taking part in the

reaction network and the term 'complex' is each one of the term appearing the at heads and tails of the reaction arrow. For instance the reaction

$$2\,\mathrm{A} + 3\,\mathrm{A{:}\,B} \longrightarrow 5\,\mathrm{A} + 3\,\mathrm{B}$$

has the species A, A:B and B and the complexes 2A + 3A:B and 5A + 3B.

With this in mind, a linear map $h : [\psi(\mathbf{S})] \longrightarrow \frac{d}{dt}\mathbf{S}$ can be established:

$$\frac{d}{dt}\mathbf{S} \quad = \quad \mathbf{Y}\mathbf{A}_k[\psi(\mathbf{S})]$$

where $\mathbf{Y}$ is the molecularity matrix, whose $ij-th$ entry is the is the stoichiometric coefficient of the $i-th$ specie in the $j-th$ complex, $\psi(\mathbf{S})$ is a vector whose components are the reaction functions of the species involved in every entry. Where:

$$\begin{aligned} \mathbf{A}_k[\psi(\mathbf{S})] &= \sum_{i=1}^{n} \psi_i(\mathbf{S}) \sum_{j \in \mathcal{I}_i} k_{ij}(\varepsilon_j - \varepsilon_i) \\ \varepsilon_{ij} &= \begin{cases} 1 & if \quad i = j \\ 0 & otherwise \end{cases} \end{aligned}$$

where $\psi_i(\mathbf{S})$ denotes the $i-th$ component of $\psi(\mathbf{S})$.

The main advantage of this modeling approach is that it has a graphical interpretation: each one of the species can be regarded as a node in a graph and each reaction as an edge. This approach is further exploited by Horn, Jackson and Feinberg (see for example, (Feinberg, 1979)), where the properties of the graph are explored in order to determine the qualitative behavior of the model. Recently, Otero-Muras (Otero-Muras et al., 2009) has used this approach to find the set of parameters where the network exhibits multistable behavior. The main drawback of the method is that strong conditions on the graph have to be complied.

2.3 Apoptosis models

In this section two different pathways and their respective models will be presented. First a general model resembling the activation of an effector caspase is introduced. Note that this simple reaction mechanism is present in both apoptosis pathways. A simplified explanation of the mechanism is given for each of the pathways and a mathematical model is presented.

2.3.1 Core reactions

The basic interaction of caspases is represented by the following set of reactions:

$$\mathcal{K}_a + \mathcal{C} \xrightarrow{\alpha} \mathcal{C}_a + \mathcal{K}_a$$
$$\mathcal{C}_a + \mathcal{K} \xrightarrow{\beta} \mathcal{K}_a + \mathcal{C}_a$$

where $\mathcal{C}$ is the initiator caspase and $\mathcal{K}$ is the effector caspase. The subindex a represents the activated version of each caspase.

The Figures 2.1-2.3 show three different caspase activation mechanisms. In these Figures, the reactants are in the tails of the arrows and the products, at the heads. The interaction of two or more reactants occur when two arrows are meeting. As can be seen in Figure 2.1, there is a positive feedback of mutual activating elements. Hence, once a single molecule of C_a is present, the whole pool of the effector caspase will be activated and the cell will eventually die. Although this model represents the basic activation of caspases, it fails to recover the robust decision in the actual process. This property of robustness is important, since a significant concentration of active caspase 3 can irreversibly cleave important proteins for the cell survival.

The mathematical model of this reaction network is:

$$\begin{pmatrix} [\dot{\mathcal{C}}] \\ [\dot{\mathcal{C}_a}] \\ [\dot{\mathcal{K}}] \\ [\dot{\mathcal{K}_a}] \end{pmatrix} = \begin{pmatrix} -1 & 0 \\ 1 & 0 \\ 0 & -1 \\ 0 & 1 \end{pmatrix} \begin{pmatrix} \alpha[\mathcal{C}][\mathcal{K}_a] \\ \beta[\mathcal{C}_a][\mathcal{K}] \end{pmatrix}$$

Note that the rank of the stoichiometric matrix is two. Hence two of the concentrations are linearly dependent, for example choose $[\mathcal{C}]$ and $[\mathcal{K}]$. Note that:

$$-[\dot{\mathcal{C}_a}] = [\dot{\mathcal{C}}] \qquad -[\dot{\mathcal{K}_a}] = [\dot{\mathcal{K}}]$$

Integrating with respect to the time:

$$[\mathcal{C}] = [\mathcal{C}_a]_0 + [\mathcal{C}]_0 - [\mathcal{C}_a] \qquad [\mathcal{K}] = [\mathcal{K}_a]_0 + [\mathcal{K}]_0 - [\mathcal{K}_a] \tag{2.2}$$

Together with the equations in (2.2) the two following ODEs fully describe the system:

$$\begin{aligned} [\dot{\mathcal{C}_a}] &= \alpha[\mathcal{C}][\mathcal{K}_a] \\ [\dot{\mathcal{K}_a}] &= \beta[\mathcal{C}_a][\mathcal{K}] \end{aligned}$$

In Figure 2.4 the dynamics of the model above are presented. Note that only 15 minutes are necessary to convert the whole pool of the initiator caspase $\mathcal{C}$ into the activated effector caspase $\mathcal{K}_a$. It is also remarkable that a relatively small initial concentration is enough to activate the mechanism.

2.3.2 Extrinsic Apoptosis Pathway (EXAP)

The simplified scheme of the process is shown in the right column of Figure 2.5.

The reactions are :

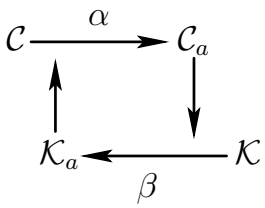

Figure 2.1: Basic interaction of caspases

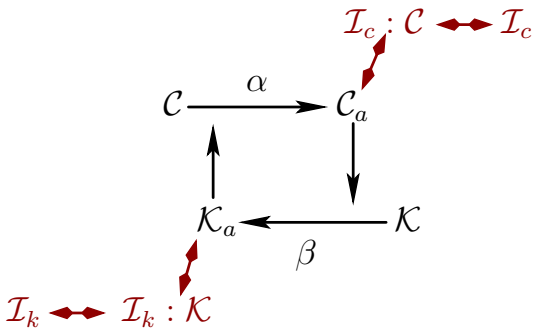

Figure 2.2: Simplified diagram of the EXAP

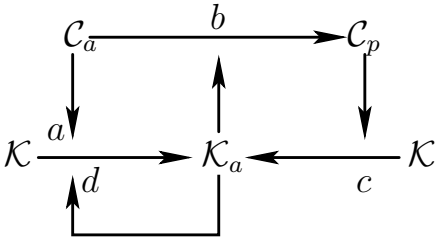

Figure 2.3: Simplified diagram of the INAP (inhibitors and activators not shown)

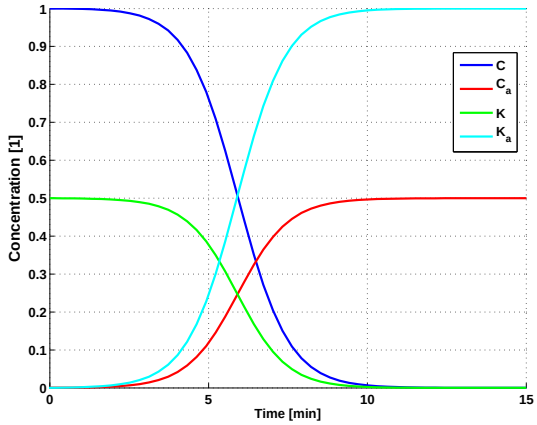

Figure 2.4: Trajectories of the states of the basic caspase interaction. The magnitude of the concentrations have been normalized using the following factors $[\mathcal{C}]_{max} = 1300000$, $[\mathcal{C}_a]_{max} = 2600000$, $[\mathcal{K}]_{max} = 42000$, $[\mathcal{K}_a]_{max} = 21000$.
The parameters used in the simulation are $\alpha = 5.8 \times 10^{-5}$ and $\beta = 10^{-5}$.
The initial conditions are:
$\mathbf{x_0} = [[\mathcal{C}]_0, [\mathcal{C}_a]_0, [\mathcal{K}]_0, [\mathcal{K}_a]_0] = [130000, 150, 21000, 0]$

$$C_{8a} + C_3 \xrightarrow{k_1} C_{3a} + C_{8a} \qquad C_{3a} + C_8 \xrightarrow{k_2} C_{8a} + C_{3a}$$

$$C_{3a} + IAP \underset{k_{m3}}{\overset{k_3}{\rightleftharpoons}} IAP : C_{3a} \qquad C_{3a} + IAP \xrightarrow{k_4} C_{3a}$$

$$C_{8a} \xrightarrow{k_5} 0 \qquad C_{3a} \xrightarrow{k_6} 0$$

$$IAP : C_{3a} \xrightarrow{k_7} 0 \qquad IAP \underset{k_{m8}}{\overset{k_8}{\rightleftharpoons}} 0$$

$$C_8 \underset{k_{m9}}{\overset{k_9}{\rightleftharpoons}} 0 \qquad C_3 \underset{k_{m10}}{\overset{k_{10}}{\rightleftharpoons}} 0$$

$$C_{8a} + CARP \underset{k_{m11}}{\overset{k_{11}}{\rightleftharpoons}} CARP : C_{8a} \qquad CARP \underset{k_{m12}}{\overset{k_{12}}{\rightleftharpoons}} 0$$

$$CARP : C_{8a} \xrightarrow{k_{13}} 0$$

As a convention, the reaction to/from zero will be understood as an efflux/influx of a substance. It can be thought of the inputs and outputs in an open reactor.

In this pathway the initiator caspase is Caspase 8 and the effector caspase is Caspase 3. CARP (Cellular Apoptosis Regulatory Protein) represents the inhibitor of C_{8a}; and IAP (Inhibitor of Apoptosis Protein), the inhibitor of C_{3a}.

In Figure 2.2 note that defining $\mathcal{C} = C_8$, $\mathcal{C}_a = C_{8a}$, $\mathcal{K} = C_3$, $\mathcal{K}_a = C_{3a}$, the core caspase activation mechanism is present in this pathway.

This model considers an initial concentration of the activated initiator caspase present ($[C_{8a}] \neq 0$), these molecules of C_{8a} can either be degraded via its inhibitor or can activate the effector caspase C_3. In turn, the C_{3a} can be either degraded by its inhibitor or can activate the initiator caspase C_8. Both IAP and CARP, inhibit the ac-

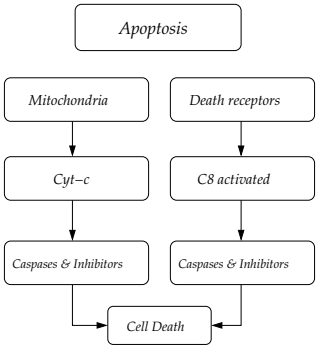

Figure 2.5: Apoptosis Pathways Schematic

tivated version of the corresponding caspase when it bonds to the activated site of the caspase, avoiding a further reaction.

In comparison to the four states model, this model has a closer behavior to the actual process, since the presence of a small concentration of the activated initiator caspase does not mean the outcome of the cell is death. Clearly, this is due to the presence of the inhibitors, since they can degrade the activated version of the respective caspase and hence make the cell immune to a certain concentration of the activated caspases. However, the pool of the inhibitors can be consumed more rapidly than its generation, thus the pool of the inhibitor eventually run out and the respective caspase will be eventually activated. It is clear that for such an important decision for the cell to reach, the mechanism has to be very precisely activated.

The dynamical model has eight states and nineteen parameters. It is build upon the Mass Action Principle, and the equations read as follows:

$$\begin{aligned}
[\dot{C_8}] &= -k_2[C_{3a}][C_8] - k_9[C_8] + k_{m9} \\
[\dot{C_{8a}}] &= k_2[C_{3a}][C_8] - k_5[C_{8a}] - k_{11}[C_{8a}][CARP] + k_{m11}[CARP : C_{8a}] \\
[\dot{C_3}] &= -k_1[C_{8a}][C_3] - k_{10}[C_3] + k_{m10} \\
[\dot{C_{3a}}] &= k_1[C_{8a}][C_3] - k_6[C_{3a}] - k_3[C_{3a}][IAP] + k_{m3}[IAP : C_{3a}] \\
[\dot{IAP}] &= k_{m3}[IAP : C_{3a}] - k_8[IAP] + k_{m8} - (k_3 + k_4)[C_{3a}][IAP] \\
[\dot{IAP : C_{3a}}] &= -(k_{m3} + k_7)[IAP : C_{3a}] + k_3[C_{3a}][IAP] \\
[\dot{CARP}] &= k_{m11}[CARP : C_{8a}] - k_{12}[CARP] + k_{m12} - k_{11}[C_{8a}][CARP] \\
[\dot{CARP : C_{8a}}] &= -(k_{m11} + k_{13})[CARP : C_{8a}] + k_{11}[C_{8a}][CARP]
\end{aligned}$$

The nominal parameters (Eissing, 2007) are presented in Table 2.1.

The phase portrait of this model with nominal parameters has three fixed points, two of them are stable nodes and one is a saddle (Bullinger, 2005) and (Dunne, 2008). Moreover, with the nominal selection of parameters the system does not seem to have any strange dynamics -chaos or limit cycles- and seems to present only two global attractors: one of them has a low concentration of C_{3a} and the other one a high concentration of C_{3a}. In the next sections, these fixed points will be referred to as the 'life'

Table 2.1: Nominal parameters for the EXAP. *Mo = Molecules

Name	Value	Units	Name	Value	Units
k_1	5.8 x 10^{-5}	$[Mo^{-1}\ min^{-1}]$	k_{10}	3.9 x 10^{-3}	$[min^{-1}]$
k_2	10^{-5}	$[Mo^{-1}\ min^{-1}]$	k_{11}	5 x 10^{-4}	$[Mo^{-1}\ min^{-1}]$
k_3	5 x 10^{-4}	$[Mo^{-1}\ min^{-1}]$	k_{12}	10^{-3}	$[min^{-1}]$
k_4	3 x 10^{-4}	$[Mo^{-1}\ min^{-1}]$	k_{13}	1.16x10^{-2}	$[min^{-1}]$
k_5	5.8 x 10^{-3}	$[min^{-1}]$	k_{m3}	0.21	$[min^{-1}]$
k_6	5.8 x 10^{-3}	$[min^{-1}]$	k_{m8}	464	$[\frac{Mo}{min}]$
k_7	1.73x 10^{-2}	$[min^{-1}]$	k_{m9}	507	$[\frac{Mo}{min}]$
k_8	1.16x 10^{-2}	$[min^{-1}]$	k_{m10}	81.9	$[\frac{Mo}{min}]$
k_9	3.9x 10^{-3}	$[min^{-1}]$	k_{m11}	0.21	$[min^{-1}]$
			k_{m12}	40	$[\frac{Mo}{min}]$

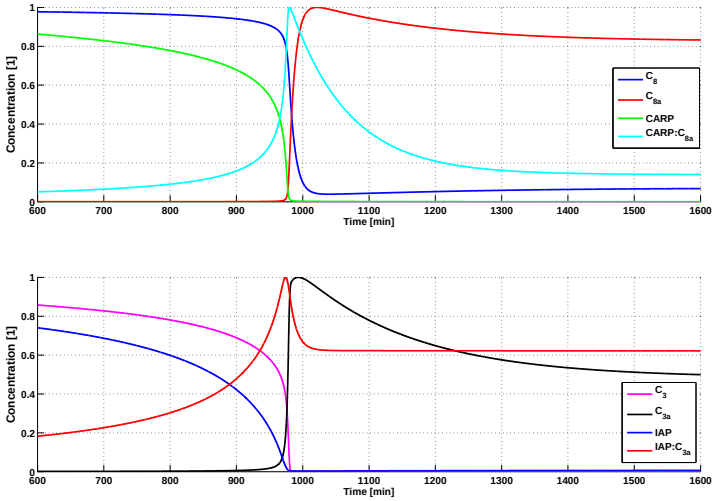

Figure 2.6: Trajectories of the states of the EXAP. The magnitude of the concentrations have been normalized to the maximum value of each of the concentrations present. $[C_8]_{max} = 1300000$, $[C_{8a}]_{max} = 89890.3$, $[C_3]_{max} = 21000$, $[C_{3a}]_{max} = 10683.9$, $[IAP]_{max} = 40000$, $[IAP : C_{3a}]_{max} = 48267$, $[CARP]_{max} = 40000$, $[CARP : C_{8a}]_{max} = 24647.2$.
The parameters used in the simulation are the nominal and the initial conditions are: $\mathbf{x_0} = [[C_8]_0, [C_{8a}]_0, [C_3]_0, [C_{3a}]_0, [IAP]_0, [IAP : C_{3a}]_0, [CARP]_0, [CARP : C_{8a}]_0] = [130000, 1000, 21000, 0, 40000, 0, 40000, 0]$

and 'death' fixed point, respectively.

It is important to note that the fixed point with a high level of C_{3a} does not have a

real biological meaning because once a high concentration of C_{3a} is reached, the cell will start to dismantle itself and the model is not longer valid. Nevertheless this model recovers the capacity of the cell to remain alive despite the presence of relatively small amounts of the initiator caspase C_{8a}. The nominal dynamics of the model are presented in Figure 2.6. Note that once the pools of the inhibitors have been consumed, the activation of caspases is almost immediately. As a matter of fact once the mechanism is activated, the dynamics are similar to the dynamics of the four states model (see Figure 2.4 on page 14). Note also that the time that the inhibitors take to degrade translates into a delay in the triggering of the mechanism.

2.3.3 Intrinsic Apoptosis Pathway (INAP)

The contents of this section are based on (Rehm et al., 2006). In the recent years the research in the INAP has been very fruitful and active. In the left column of Figure 2.5 on page 15 a simplified diagram of the activation mechanism of this pathway is presented. Note that the name of this pathway relies on the origin of the triggering signal of the mechanism. A more detailed explanation of the process is presented below.

The mitochondria are one of the organelles of the eukariotic cells which regulate several processes of the cell and carry out the important oxidation of food molecules (Alberts et al., 2002). In the INAP, the activation of the effector caspases is triggered by an input signal to the mitochondria and the subsequent release of proteins which promote apoptosis. The release of cytochrome c (*cyt-c*) triggers the formation of the apoptosome, a multiprotein complex whose bound with Caspase 9 activates the effector Caspases 3 and 7 . As in the EXAP, the presence of inhibitors (IAP) counteract the activation of the caspases. However, the mitochondria also releases an activator of the process, whose role is the inhibition of IAP, promoting the final activation of the effector caspases. This activator is referred in the literature as Smac or DIABLO. The formation of the apoptosome is also regulated by the BIR.

The basic interaction of Caspases for this model is presented in Figure 2.3 and the whole set of equations can be splited as follows.

The basic interaction of caspases in this pathway is represented by the reactions:

$$C_{9a} + C_3 \xrightarrow{k_5} C_{9a} + C_{3a}$$
$$C_{9a} + C_{3a} \xrightarrow{k_6} C_{9p} + C_{3a}$$
$$C_{9p} + C_3 \xrightarrow{k_7} C_{9p} + C_{3a}$$
$$C_3 + C_{3a} \xrightarrow{k_8} 2\,C_{3a}$$

Note from Figure 2.3 and the aforementioned reactions that the basic interaction of caspases has been modeled to present autoactivation of C_{3a}.

The reactions of XIAP and the caspases are:

$$C_{3a} + XIAP \xrightarrow{k_9} XIAP : C_{3a}$$
$$XIAP : C_{3a} \xrightarrow{k_{10}} C_{3a} + XIAP$$
$$C_{3a} + XIAP : C_{9a} \xrightarrow{k_{11}} XIAP : C_{9a}C_{3a}$$
$$XIAP : C_{9a}C_{3a} \xrightarrow{k_{12}} C_{3a} + XIAP : C_{9a}$$
$$C_{3a} + XIAPp2frag \xrightarrow{k_{13}} XIAPp2frag : C_{3a}$$
$$XIAPp2frag : C_{3a} \xrightarrow{k_{14}} C_{3a} + XIAPp2frag$$
$$C_{3a} + XIAP \xrightarrow{k_{17}} Bir12 + Bir3R + C_{3a}$$

$C_{3a} + XIAP : C_{9a} \xrightarrow{k_{18}} Bir12 + Bir3R : C_{9a} + C_{3a}$
$C_{3a} + XIAP : C_{3a} \xrightarrow{k_{19}} Bir3R + Bir12 : C_{3a} + C_{3a}$
$C_{3a} + XIAPp2frag \xrightarrow{k_{20}} C_{3a} + Bir12 + Bir3Rp2frag$
$C_{3a} + XIAPp2frag : C_{3a} \xrightarrow{k_{21}} C_{3a} + Bir12 : C_{3a} + Bir3Rp2frag$
$C_{3a} + XIAP : C_{9a}C_{3a} \xrightarrow{k_{22}} C_{3a} + Bir12 : C_{3a} + Bir3R : C_{9a}$
$C_{3a} + XIAP : 2Smac \xrightarrow{k_{23}} C_{3a} + Bir12 : Smac + Bir3R : Smac$
$C_{3a} + XIAP : C_{9a}C_{3a} \xrightarrow{k_{24}} C_{3a} + C_{9p} + XIAPp2frag : C_{3a}$
$C_{3a} + XIAP : C_{9a} \xrightarrow{k_{25}} C_{3a} + C_{9p} + XIAPp2frag$
$C_{3a} + Bir3R : C_{9a} \xrightarrow{k_{26}} C_{3a} + Bir3Rp2frag + C_{9p}$
$C_{9a} + XIAP \xrightarrow{k_{27}} XIAP : C_{9a}$
$XIAP : C_{9a} \xrightarrow{k_{28}} C_{9a} + XIAP$
$C_{9a} + XIAP : C_{3a} \xrightarrow{k_{29}} XIAP : C_{9a} : C_{3a}$
$XIAP : C_{9a} : C_{3a} \xrightarrow{k_{30}} C_{9a} + XIAP : C_{3a}$
$XIAPp2frag \xrightarrow{k_{34}} XIAP$
$XIAP + 2Smac \xrightarrow{k_{35}} XIAP : 2Smac$
$XIAP : 2Smac \xrightarrow{k_{36}} XIAP + 2Smac$
$XIAP : C_{9a} + 2Smac \xrightarrow{k_{37}} XIAP : 2Smac + C_{9a}$
$XIAP : 2Smac + C_{9a} \xrightarrow{k_{38}} XIAP : C_{9a} + 2Smac$
$XIAP : C_{3a} + 2Smac \xrightarrow{k_{39}} XIAP : 2Smac + C_{3a}$
$XIAP2Smac + C_{3a} \xrightarrow{k_{40}} XIAP : C_{3a} + 2Smac$
$XIAP : C_{9a} : C_{3a} + 2Smac \xrightarrow{k_{41}} XIAP : 2Smac + C_{3a} + C_{9p}$
$XIAP : 2Smac + C_{3a} + C_{9p} \xrightarrow{k_{42}} XIAP : C_{9a} : C_{3a} + 2Smac$
$XIAPp2frag + 2Smac \xrightarrow{k_{51}} XIAPp2frag : 2Smac$
$XIAPp2frag : 2Smac \xrightarrow{k_{52}} XIAPp2frag + 2Smac$

The regulation effect of the BIR is represented by the reactions:

$C_{3a} + Bir12 \xrightarrow{k_{15}} Bir12 : C_{3a}$
$Bir12 : C_{3a} \xrightarrow{k_{16}} C_{3a} + Bir12$
$C_{9a} + Bir3R \xrightarrow{k_{31}} Bir3R : C_{9a}$
$Bir3R : C_{9a} \xrightarrow{k_{32}} C_{9a} + Bir3R$
$Bir3Rp2frag \xrightarrow{k_{33}} Bir3R$
$Bir12 + Smac \xrightarrow{k_{43}} Bir12 : Smac$
$Bir12 : Smac \xrightarrow{k_{44}} Bir12 + Smac$
$Bir3R + Smac \xrightarrow{k_{45}} Bir3R : Smac$
$Bir3R : Smac \xrightarrow{k_{46}} Bir3R + Smac$
$Bir12 : C_{3a} + Smac \xrightarrow{k_{47}} Bir12 : Smac + C_{3a}$
$Bir12 : Smac + C_{3a} \xrightarrow{k_{48}} Bir12 : C_{3a} + Smac$
$Bir3R : C_{9a} + Smac \xrightarrow{k_{49}} Bir3R : Smac + C_{9a}$
$Bir3R : Smac + C_{9a} \xrightarrow{k_{50}} Bir3R : C_{9a} + Smac$

The influx and degradation of the different reactants, with:

$C_3 \xrightarrow{k_1} 0$
$0 \xrightarrow{k_2} C_3$
$XIAP \xrightarrow{k_3} 0$
$0 \xrightarrow{k_4} XIAP$

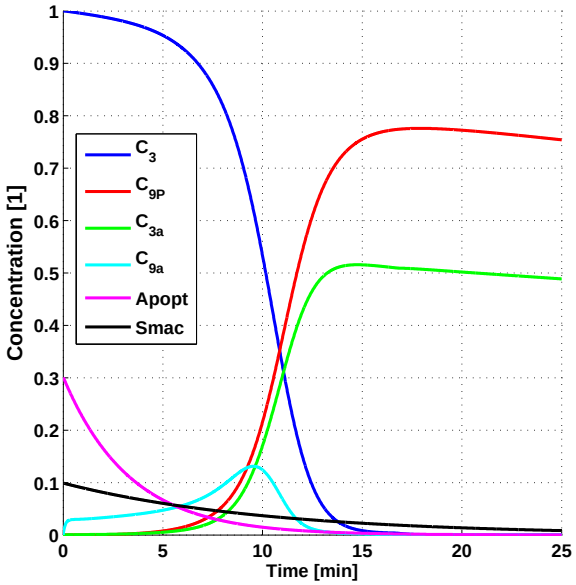

Figure 2.7: Trajectories of the states of the INAP. The magnitude of the concentrations have been normalized according with the next factors: $[C_3], [C_{3a}] \rightarrow 0.12$; $[C_{9P}], [C_{9a}], [Apotosome] \rightarrow 0.03$ and $[Smac] \rightarrow 0.126$ The parameters used in the simulation are the nominal and the initial conditions are all zero except for $[C_3]_0 = 0.12$ and $[IAP]_0 = 0.0603$.

$C_{9p} \xrightarrow{k_{53}} 0$
$C_{9a} \xrightarrow{k_{54}} 0$
$C_{3a} \xrightarrow{k_{55}} 0$
$XIAP : C_{3a} \xrightarrow{k_{56}} 0$
$XIAP : C_{9a}C_{3a} \xrightarrow{k_{57}} 0$
$XIAP : C_{9a} \xrightarrow{k_{58}} 0$
$XIAPp2frag \xrightarrow{k_{59}} 0$
$XIAPp2frag : C_{3a} \xrightarrow{k_{60}} 0$
$XIAPp2frag : 2Smac \xrightarrow{k_{61}} 0$
$XIAP : 2Smac \xrightarrow{k_{62}} 0$
$Bir12 \xrightarrow{k_{63}} 0$
$Bir3R \xrightarrow{k_{64}} 0$
$Bir1 : 2Smac \xrightarrow{k_{65}} 0$
$Bir3R : Smac \xrightarrow{k_{66}} 0$
$Bir12 : C_{3a} \xrightarrow{k_{67}} 0$
$Bir3R : C_{9a} \xrightarrow{k_{68}} 0$
$Bir3Rp2frag \xrightarrow{k_{69}} 0$
$Smac \xrightarrow{k_{70}} 0$

The reactions presented above reproduce the process from the release of *cyt-c* to the final activation of the effector caspase. The set of ODEs that represents the model is presented in Appendix B and the nominal parameters are shown in Table 2.2. Finally, Figure 2.7 shows some of the trajectories of the relevant states.

Table 2.2: Nominal parameters for the INAP

Name	Value	Units	Name	Value	Units
k_1	0.0039	$[min^{-1}]$	k_{36}	0.133	$[min^{-1}]$
k_2	$k_1 C_{3ini}$	$[\mu M^{-1} min^{-1}]$	k_{37}	420	$[\mu M^{-2} min^{-1}]$
k_3	0.0116	$[min^{-1}]$	k_{38}	156	$[\mu M^{-1} min^{-1}]$
k_4	$k_3 XIAP_{init}$	$[\mu M^{-1} min^{-1}]$	k_{39}	420	$[\mu M^{-2} min^{-1}]$
k_5	6	$[\mu M^{-1} min^{-1}]$	k_{40}	156	$[\mu M^{-1} min^{-1}]$
k_6	12	$[\mu M^{-1} min^{-1}]$	k_{41}	0	-
k_7	48	$[\mu M^{-1} min^{-1}]$	k_{42}	0	-
k_8	2.4	$[\mu M^{-1} min^{-1}]$	k_{43}	4.45	$[\mu M^{-1} min^{-1}]$
k_9	156	$[\mu M^{-1} min^{-1}]$	k_{44}	31.9	$[min^{-1}]$
k_{10}	0.1440	$[min^{-1}]$	k_{45}	0.33	$[\mu M^{-1} min^{-1}]$
k_{11}	0	-	k_{46}	14.2	$[min^{-1}]$
k_{12}	0	-	k_{47}	4.45	$[\mu M^{-1} min^{-1}]$
k_{13}	0	-	k_{48}	156	$[\mu M^{-1} min^{-1}]$
k_{14}	0	-	k_{49}	0.3300	$[\mu M^{-1} min^{-1}]$
k_{15}	156	$[\mu M^{-1} min^{-1}]$	k_{50}	156	$[\mu M^{-1} min^{-1}]$
k_{16}	0.1440	$[min^{-1}]$	k_{51}	420	$[\mu M^{-2} min^{-1}]$
k_{17}	12	$[\mu M^{-1} min^{-1}]$	k_{52}	156	$[\mu M^{-1} min^{-1}]$
k_{18}	12	$[\mu M^{-1} min^{-1}]$	k_{53}	0.0058	$[min^{-1}]$
k_{19}	12	$[\mu M^{-1} min^{-1}]$	k_{54}	0.0058	$[min^{-1}]$
k_{20}	12	$[\mu M^{-1} min^{-1}]$	k_{55}	0.0058	$[min^{-1}]$
k_{21}	12	$[\mu M^{-1} min^{-1}]$	k_{56}	0.0347	$[min^{-1}]$
k_{22}	12	$[\mu M^{-1} min^{-1}]$	k_{57}	0.0347	$[min^{-1}]$
k_{23}	12	$[\mu M^{-1} min^{-1}]$	k_{58}	0.0347	$[min^{-1}]$
k_{24}	12	$[\mu M^{-1} min^{-1}]$	k_{59}	0.0058	$[min^{-1}]$
k_{25}	12	$[\mu M^{-1} min^{-1}]$	k_{60}	0.0347	$[min^{-1}]$
k_{26}	12	$[\mu M^{-1} min^{-1}]$	k_{61}	0.0347	$[min^{-1}]$
k_{27}	156	$[\mu M^{-1} min^{-1}]$	k_{62}	0.0347	$[min^{-1}]$
k_{28}	0.1440	$[min^{-1}]$	k_{63}	0.0058	$[min^{-1}]$
k_{29}	0	-	k_{64}	0.0347	$[min^{-1}]$
k_{30}	0	-	k_{65}	0.0058	$[min^{-1}]$
k_{31}	156	$[\mu M^{-1} min^{-1}]$	k_{66}	0.0347	$[min^{-1}]$
k_{32}	0.1440	$[min^{-1}]$	k_{67}	0.0058	$[min^{-1}]$
k_{33}	0	-	k_{68}	0.0058	$[min^{-1}]$
k_{34}	0	-	k_{69}	0.0347	$[min^{-1}]$
k_{35}	420	$[\mu M^{-2} min^{-1}]$	k_{70}	0.0058	$[min^{-1}]$

Chapter 3

Steady State Analysis and Structure Identification

Introduction

In general, dynamic models of cellular signalling pathways are complex and tightly regulated. The network of reactions present in a pathway can be interpreted as a chain of reactions endowed with regulators. As a result, every reaction can influence the rest of the network at the appropriate time and amount. In this work, based on a deterministic representation of the pathway, a methodology for a systematic approach to identify the building blocks of the network is presented, as a technique for coping with the complexity of the network. A further analysis of the identified subsystems can define their role in the network, thus giving insight to the network. The outline of the proposed methodology reads as follows: in the context of Graph Theory, a reduction of the incidence matrix bandwidth via the reverse Cuthill-McKee algorithm is done (Cuthill, 1969). The analysis of the identified subsystems is performed, resulting in the identification of the controller of the network. In Chapter 5 robustness analysis is applied in both dynamical models to characterize the characteristic properties of the networks.

3.1 Extrinsic Apoptosis Pathway

3.1.1 Plant-Controller Scheme in the Extrinsic Apoptosis Pathway

As introduced in Chapter 2 the model of the extrinsic Apoptosis pathway (Eissing, 2007) is presented in Equation 3.1.

$$
\begin{array}{rl|l}
\dot{[C_8]} = & -k_2[C_{3a}][C_8] - k_9[C_8] + k_{m9} & \\
\dot{[C_{8a}]} = & k_2[C_{3a}][C_8] - k_5[C_{8a}] & -k_{11}[C_{8a}][CARP] + k_{m11}[CARP : C_{8a}] \\
\dot{[C_3]} = & -k_1[C_{8a}][C_3] - k_{10}[C_3] + k_{m10} & \\
\dot{[C_{3a}]} = & k_1[C_{8a}][C_3] - k_6[C_{3a}] & -k_3[C_{3a}][IAP] + k_{m3}[IAP : C_{3a}] \\
\dot{[IAP]} = & k_{m3}[IAP : C_{3a}] - k_8[IAP] + k_{m8} & -(k_3 + k_4)[C_{3a}][IAP] \\
\dot{[IAP : C_{3a}]} = & -(k_{m3} + k_7)[IAP : C_{3a}] & k_3[C_{3a}][IAP] \\
\dot{[CARP]} = & k_{m11}[CARP : C_{8a}] - k_{12}[CARP] + k_{m12} & -k_{11}[C_{8a}][CARP] \\
\dot{[CARP : C_{8a}]} = & -(k_{m11} + k_{13})[CARP : C_{8a}] & k_{11}[C_{8a}][CARP]
\end{array}
\tag{3.1}
$$

Note that the separation presented in the model, which at first glimpse may seem arbitrary, reflects an important property of the network. The first four differential equations are function almost solely of the variables which appear differentiated, i.e., these first four equations can be regarded as a system with two exogenous input signals (the remaining terms).The very same analogy can be done for the last four equations.
In this context, (3.1) can be written as the interconnection of two systems: the interaction among the caspases and the interactions due to the presence of the inhibitors (Figure 3.1). Let this former system be called the plant and the inhibitor's differential equations, the regulator. A closer look to (3.1) shows that this same idea can be performed again in the plant and the controller, that is to say, the four differential equations in the plant can be splited again into two subsystems: the activation of Caspase 3 (third and fourth equation) and Caspase 8 (first and second equation). Even more important, the controller can be decomposed in a similar way and the "input" to each controller is only one of the activated caspases. The regulator presented in Figure (3.1) is *decentralized* (see Figure 3.2). Note that: i) the controllers can be thought as output controllers and ii) the four subsystems are nonlinear SISO, namely:

$$\mathcal{P}_1 : \begin{cases} [\dot{C_8}] &= -k_2[C_{3a}][C_8] - k_9[C_8] + k_{m9} \\ [\dot{C_{8a}}] &= k_2[C_{3a}][C_8] - k_5[C_{8a}] \underbrace{-k_{11}[C_{8a}][CARP] + k_{m11}[CARP : C_{8a}]}_{u_1} \end{cases}$$

$$\mathcal{K}_1 : \begin{cases} [\dot{CARP}] &= k_{m11}[CARP : C_{8a}] - k_{12}[CARP] + k_{m12} - k_{11} \overbrace{[C_{8a}]}^{v_1 = y_1}[CARP] \\ [\dot{CARP : C_{8a}}] &= -(k_{m11} + k_{13})[CARP : C_{8a}] + k_{11}[C_{8a}][CARP] \end{cases}$$

$$\mathcal{P}_2 : \begin{cases} [\dot{C_3}] &= -k_1[C_{8a}][C_3] - k_{10}[C_3] + k_{m10} \\ [\dot{C_{3a}}] &= k_1[C_{8a}][C_3] - k_6[C_{3a}] \underbrace{-k_3[C_{3a}][IAP] + k_{m3}[IAP : C_{3a}]}_{u_2} \end{cases}$$

$$\mathcal{K}_2 : \begin{cases} [\dot{IAP}] &= k_{m3}[IAPC_{3a}] - k_8[IAP] + k_{m8} - (k_3 + k_4) \overbrace{[C_{3a}]}^{v_2 = y_2}[IAP] \\ [\dot{IAP : C_{3a}}] &= -(k_{m3} + k_7)[IAP : C_{3a}] + k_3[C_{3a}][IAP] \end{cases}$$

Note also that the nomenclature present in the definitions above is in accordance with the Figure 3.2 and the election of the output of each system is the activated caspase. Note also that the output of each plant is the input to its respective controller and the next plant, i.e., $y_1 = v_1 = w_2$ and $y_2 = v_2 = w_1$. Note that Figure 3.2 can be simplified, since the signals $y_i = v_i$ are the same, but keeping this structure intends to emphasize the decoupling of the dynamics.

In order to perform the previous decoupling, an heuristic approach was used. Nev-

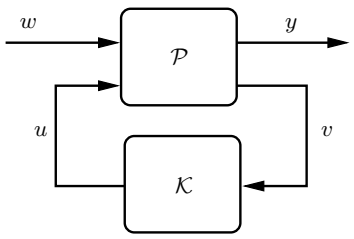

Figure 3.1: A general controlled system

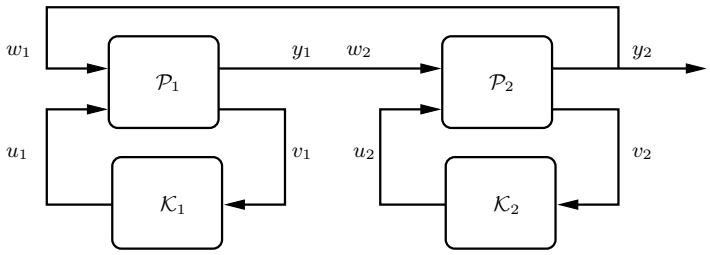

Figure 3.2: Block diagram representation for the EXAP

ertheless, a systematic approach can be adopted as follows. Let:

$$l_{ij} \quad = \quad \begin{cases} 1 & , \quad J_{ij} \neq 0 \\ 0 & , \quad J_{ij} = 0 \end{cases} \tag{3.2}$$

where $\mathcal{J} \equiv \{J_{ij}\}$ is the Jacobian of the full system (3.1) and the element l_{ij} shows the dependence of the i-th differential equation upon the j-th variable, i.e. $\mathcal{L} \equiv \{l_{ij}\}$ is the incidence matrix . In order to isolate the subsystems, consider the ordering of $\mathcal{L}$ after applying the reverse Cuthill-McKee algorithm (Cuthill and McKee, 1969) to $\mathcal{L}$, which is in essence a reordering of the matrix's rows and columns such that the biggest quantity of nonzero elements lie the closest to the principal diagonal as possible. For a formal statement of the problem, see Appendix A. In order to keep some biochemical sense, a rearrangement of this set up can be done. Figure 3.3 shows this rearrangement for the incidence matrix $\mathcal{L}$ of the system (3.1). In Figure 3.3, the functional form of the

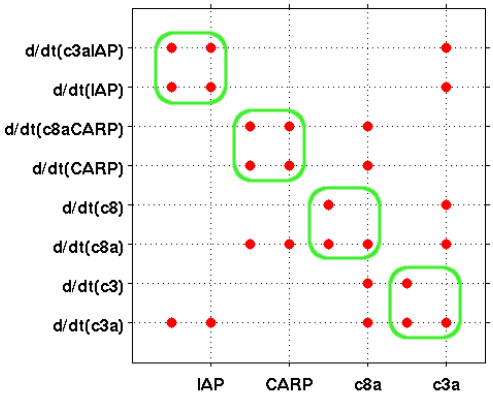

Figure 3.3: Sparse Graph of the EXAP model.
The boxes represent a subsystem and the dots out of them, interconnection signals among the systems.

inputs and the outputs is not shown, but only the dependence itself.

Once decomposed, the main question is what are the essential interconnection properties of the blocks such that the robust bistable properties hold. Under which sets of parameters the evolution of C_{3a} is bistable? What are the key reactions? The answers to these questions are considered in the following chapters. In the next section a simple steady state analysis will be carried out.

3.1.2 Steady State analysis

Let the system

$$\begin{aligned} \dot{x}_1^i &= -(k_{ai}w_i + k_{ci})x_1^i + k_{mci} \\ \dot{x}_2^i &= k_{ai}w_i x_1^i - k_{cai}x_2^i + u_i \\ y^i &= x_2^i = v_i \end{aligned} \tag{3.3}$$

represent the plant $\mathcal{P}_1$ with $x^1 \equiv (C_8, C_{8a})^T$ and $\mathcal{P}_2$ with $x^2 \equiv (C_3, C_{3a})^T$. The parameters for each system are listed in Table 3.1.

Note that the same property holds for the regulators $\mathcal{K}_1$ and $\mathcal{K}_2$ and let the system representing them, to be as follows:

$$\begin{aligned} \dot{z}_1^i &= -[(k_{ri} + k_{rbi})v_i + k_{ni}]z_1^i + k_{mri}z_2^i + k_{mni} \\ \dot{z}_2^i &= k_{ri}v_i z_1^i - (k_{mri} + k_{cni})z_2^i \\ u_i &= -k_{ri}v_i z_1^i + k_{mri}z_2^i \end{aligned} \tag{3.4}$$

where $z^1 \equiv ([CARP], [CARP : C_{8a}])$ and $z^2 \equiv ([IAP], [IAP : C_{3a}])$. In the following the index i will be omitted for readability, except when the analysis of both plants is being performed.

It is important to note that both the states and the parameters in the two systems above can only have positive values. In the following sections, a steady state analysis

Table 3.1: Parameter definition for the EXAP

$\mathcal{P}_1 - \mathcal{K}_1$	$\mathcal{P}_2 - \mathcal{K}_2$	Label	Velocity parameter of the reaction
k_2	k_1	k_a	Activation of caspase
k_5	k_6	k_{ca}	Activated caspase degradation
k_9, k_{m9}	k_{10}, k_{m10}	k_c, k_{mc}	Caspase turnover
k_{12}, k_{m12}	k_8, k_{m8}	k_n, k_{mn}	Inhibitor turnover
k_{11}, k_{m11}, k_{11b}	k_3, k_{m3}, k_4	k_r, k_{mr}, k_{rb}	Reversible reaction
k_{13}	k_7	k_{cn}	Degradation of the complex Caspase : Inhibitor

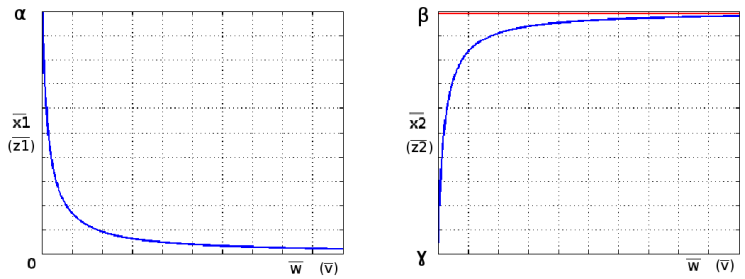

Figure 3.4: Equilibria loci of the open loop plant (regulator)

will be performed to the plant $\mathcal{P}_i$, the regulator $\mathcal{K}_i$, the interconnection of the plant and the controller (denoted by $\mathcal{P}_i - \mathcal{K}_i$) and finally the interconnections of both plants and controllers.

Plant

The fixed point of (3.3) is:

$$\begin{aligned} \bar{x}_1 &= \frac{k_{mc}}{k_c + k_a \bar{w}} \\ \bar{x}_2 &= \frac{k_a k_{mc} \bar{w}}{k_{ca}(k_c + k_a \bar{w})} + \frac{1}{k_{ca}} \bar{u} \end{aligned} \tag{3.5}$$

Figure (3.4) presents the locus of the fixed point as a function of $(\bar{w}, \bar{u})$, with $\alpha = k_{mc}/k_c$, $\beta = (k_{mc} + \bar{u})/k_{ca}$ and $\gamma = \bar{u}/k_{ca}$.

Remark 3.1.

The pair $(\bar{x}_1, \bar{x}_2)$ is unique for each $(\bar{w}, \bar{u})$, see the Equation (3.5) and Figure 3.4.

Claim 3.1. *Let the deviation from the fixed point be represented by $\mathbf{e} \equiv \mathbf{x} - \bar{\mathbf{x}}$. Its evolution in time is determined by:*

$$\begin{pmatrix} \dot{e}_1 \\ \dot{e}_2 \end{pmatrix} = \begin{pmatrix} -(k_a \bar{w} + k_c) & 0 \\ k_a \bar{w} & -k_{ca} \end{pmatrix} \begin{pmatrix} e_1 \\ e_2 \end{pmatrix} \tag{3.6}$$

Then, regarding $\bar{w}$ as a parameter, (3.6) is linear and stable for $\bar{w} \in \left(-\frac{k_c}{k_a}, \infty\right)$.

Proof. The proof is straightforward since the system is lower-diagonal. □

Remark 3.2. *Recall (3.3) is the model of a chemical reaction network.*

i Since w is a concentration it is always positive and hence (3.6) is always steady-state stable.

ii Since $\mathbf{p} \in \Re^p$, the eigenvalues are real numbers. Hence the fixed point is a node.

iii The input u does not affect the stability of (3.6), yet determines the location of the fixed point of (3.3)

Regulator

As in the previous analysis, let the model of both regulators be represented by:

$$\begin{aligned} \dot{z}_1 &= -[(k_r + k_{rb})v + k_n]z_1 + k_{mr}z_2 + k_{mn} \\ \dot{z}_2 &= k_r v z_1 - (k_{mr} + k_{cn})z_2 \\ u &= -k_r v z_1 + k_{mr} z_2 \end{aligned} \tag{3.7}$$

whose unique fixed point is:

$$\begin{aligned} \bar{z}_1 &= \frac{(k_{cn} + k_{mr})\, k_{mn}}{k_n\,(k_{cn} + k_{mr}) + (k_r k_{cn} + k_{rb}(k_{mr} + k_{cn}))\,\bar{v}} \\ \bar{z}_2 &= \frac{k_r k_{mn} \bar{v}}{k_n\,(k_{cn} + k_{mr}) + (k_r k_{cn} + k_{rb}(k_{mr} + k_{cn}))\,\bar{v}} \end{aligned} \tag{3.8}$$

Despite the complexity of the previous expressions, they have the same functional form as (3.5). Thus Figure 3.4 also represents the equilibrium loci for the regulator with the definition of $\alpha = k_{mn}/k_n$, $\beta = [k_r k_{mn}]/[k_n\,(k_{cn} + k_{mr}) + (k_r k_{cn} + k_{rb}(k_{mr} + k_{cn}))]$ and $\gamma = 0$.

Claim 3.2. *Let $\mathbf{r} \equiv \mathbf{z} - \bar{\mathbf{z}}$, being its the evolution in time:*

$$\begin{pmatrix} \dot{r}_1 \\ \dot{r}_2 \end{pmatrix} = \begin{pmatrix} -\left((k_r + k_{rb})\bar{v} + k_n\right) & k_{mr} \\ \bar{v} k_r & -(k_{cn} + k_{mr}) \end{pmatrix} \begin{pmatrix} r_1 \\ r_2 \end{pmatrix} \tag{3.9}$$

Assuming v as a parameter, (3.9) is a linear stable system.

Proof. The characteristic polynomial of (3.9) is:

$$s^2 + s\,[(k_r + k_{rb})\bar{v} + k_n + k_{cn} + k_{mr}] + [(k_r + k_{rb})\bar{v} + k_n]\,[k_{cn} + k_{mr}] + k_{mr} k_r \bar{v} = 0$$

From the Routh criterion, the stability of (3.9) is guaranteed for:

$$\bar{v} > max\left\{ -\frac{k_n + k_{cn} + k_{mr}}{k_r + k_{rb}}, -\frac{k_n\,[k_{cn} + k_{mr}]}{[k_r + k_{rb}]\,[k_{cn} + k_{mr}] + k_r k_{mr}} \right\} \tag{3.10}$$

Since v is a concentration, it is positive. So this condition is always satisfied and the claim is proven. □

In order to precise the regulator's action on the plant, consider the next proposition.

Proposition 3.1. *Let $\mathcal{W}$ be the reaction network described by the reactions*

$$\mathcal{C}_a + \mathcal{I} \underset{v_-}{\overset{v_+}{\rightleftharpoons}} \mathcal{C}_a : \mathcal{I}$$
$$\mathcal{C}_a \xrightarrow{k_c} 0$$
$$\mathcal{I} \xrightarrow{k_i} 0$$
$$\mathcal{C}_a : I \xrightarrow{k_{ci}} 0$$

Then $[\mathcal{C}_a]$ $([\mathcal{I}])$ *is controlled by the function*

$$u = \frac{d}{dt}[\mathcal{C}_a : \mathcal{I}] + k_{ci}[\mathcal{C}_a : \mathcal{I}] \equiv \mathcal{P}\partial_{k_{ci}}\{[\mathcal{C}_a : \mathcal{I}]\}$$

That is to say, the regulator is a classical Proportional Derivative (PD) controller .

Proof. Let $v = v_+ - v_-$. The mathematical model of $\mathcal{W}$ is:

$$\begin{aligned}
\frac{d}{dt}[\mathcal{C}_a] &= -v - k_c[\mathcal{C}_a] \\
\frac{d}{dt}[\mathcal{I}] &= -v - k_i[\mathcal{I}] \\
\frac{d}{dt}[\mathcal{C}_a : \mathcal{I}] &= v - k_{ci}[\mathcal{C}_a : \mathcal{I}]
\end{aligned}$$

let $u = \frac{d}{dt}[\mathcal{C}_a : \mathcal{I}] + k_{ci}[\mathcal{C}_a : \mathcal{I}] \equiv \mathcal{P}\partial_{k_{ci}}\{[\mathcal{C}_a : \mathcal{I}]\} = v$, then $\mathcal{W}$ becomes

$$\begin{aligned}
\frac{d}{dt}[\mathcal{C}_a] &= -u - k_c[\mathcal{C}_a] \\
\frac{d}{dt}[\mathcal{I}] &= -u - k_i[\mathcal{I}]
\end{aligned}$$

Then u can be regarded as an input to the concentration of $\mathcal{C}_a$ $(\mathcal{I})$. For a block diagram of this scheme, see Figure 3.5. □

Remark 3.3. *Note that:*

- *The last proposition is valid regardless of the assignation of the reaction mechanism to the network*
- *This reaction network leads to a negative feedback scheme*
- $[\mathcal{C}_a : \mathcal{I}]$ *can be considered as an error signal.*

Claim 3.3. *The regulator* $\mathcal{R}_i$ *is a proportional derivative controller.*

Proof. Note from the reaction mechanism (in Section 2.3.2) in $\mathcal{R}_i$ has the same reactions as $\mathcal{W}$ in Proposition 3.1.

□

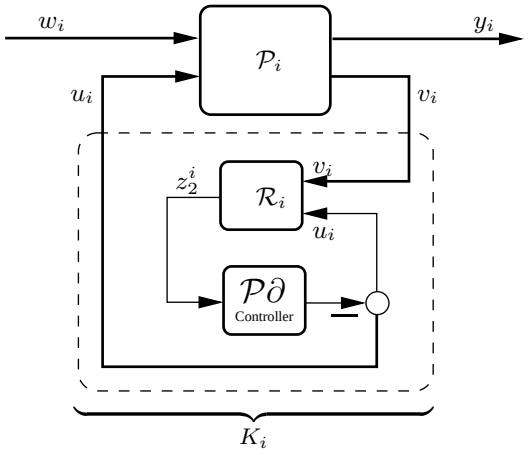

Figure 3.5: PD controller structure, where the subindex $_i$ stands for each of the subsystems.

Remark 3.4. *(3.7 on page 26) can be rewritten in the following way (see Figure 3.5).*

$$\mathcal{R}: \begin{cases} \dot{z}_1 &= -k_n z_1 + k_{mn} + u \\ \dot{z}_2 &= k_r v z_1 - (k_{mr} + k_{cn}) z_2 \end{cases}$$
$$u = -\left(k_{cn} z_2 + \frac{d}{dt} z_2 \right)$$

Closed Loop

Claim 3.4. *Consider the interconnection of $\mathcal{P}_i$ (3.3) and $\mathcal{K}_i$ (3.4):*

$$\begin{aligned} \dot{x}_1 &= -(k_a w + k_c) x_1 + k_{mc} \\ \dot{x}_2 &= k_a w x_1 - k_{ca} x_2 - k_r x_2 z_1 + k_{mr} z_2 \\ \dot{z}_1 &= -[(k_r + k_{rb}) x_2 + k_n] z_1 + k_{mr} z_2 + k_{mn} \\ \dot{z}_2 &= k_r x_2 z_1 - (k_{mr} + k_{cn}) z_2 \end{aligned}$$

The fixed point of this interconnection is:

$$\begin{aligned}
\bar{x}_1 &= \frac{k_{mc}}{k_c + k_a\bar{w}} \\
\bar{x}_2 &= \frac{1}{2}\left[-b(\bar{w}) + \sqrt{b^2(\bar{w}) + 4c(\bar{w})}\right] \\
\bar{z}_1 &= \frac{(k_{cn} + k_{mr})\, k_{mn}}{k_n\,(k_{cn} + k_{mr}) + (k_r k_{cn} + k_{rb}(k_{mr} + k_{cn}))\,\bar{x}_2} \\
\bar{z}_2 &= \frac{k_r k_{mn}\bar{x}_2}{\underbrace{k_n\,(k_{cn} + k_{mr})}_{d_1} + \underbrace{(k_r k_{cn} + k_{rb}(k_{mr} + k_{cn}))}_{d_2}\,\bar{x}_2}
\end{aligned}$$

where b and c are defined in (3.12) and (3.13), respectively.

Proof. Solving (3.11), the fixed points satisfy:

$$\begin{aligned}
\bar{x}_1 &= \frac{k_{mc}}{k_c + k_a\bar{w}} \\
\bar{x}_2 &= \frac{k_a\bar{w}}{k_{ca} + k_r\bar{z}_1}\bar{x}_1 + \frac{k_{mr}}{k_{ca} + k_r\bar{z}_1}\bar{z}_2 \\
\bar{z}_1 &= \frac{k_{mr}}{k_n + (k_r + k_{rb})\bar{x}_2}\bar{z}_2 + \frac{k_{mn}}{k_n + (k_r + k_{rb})\bar{x}_2} \\
\bar{z}_2 &= \frac{k_r\bar{x}_2}{k_{mr} + k_{cn}}\bar{z}_1
\end{aligned} \tag{3.11}$$

From (3.5) $\bar{x}_1$ and form (3.8) $\bar{z}_1$, $\bar{z}_2$ are:

$$\begin{aligned}
\bar{x}_1 &= \frac{k_{mc}}{k_c + k_a\bar{w}} \\
\bar{z}_1 &= \frac{(k_{cn} + k_{mr})\, k_{mn}}{k_n\,(k_{cn} + k_{mr}) + (k_r k_{cn} + k_{rb}(k_{mr} + k_{cn}))\,\bar{x}_2} = \frac{(k_{cn} + k_{mr})\, k_{mn}}{d_1 + d_2\bar{x}_2} \\
\bar{z}_2 &= \frac{k_r k_{mn}\bar{x}_2}{\underbrace{k_n\,(k_{cn} + k_{mr})}_{d_1} + \underbrace{(k_r k_{cn} + k_{rb}(k_{mr} + k_{cn}))}_{d_2}\,\bar{x}_2} = \frac{k_r k_{mn}\bar{x}_2}{d_1 + d_2\bar{x}_2}
\end{aligned}$$

Replacing them in $\bar{x}_2$:

$$\bar{x}_2^2 + b\bar{x}_2 - c = 0$$

Where

$$b \equiv (k_{ca}d_2)^{-1}\left[k_a k_n(k_{cn} + k_{mr}) + k_r k_{mn} k_{cn} - \frac{d_2 k_a k_{mc}\bar{w}}{k_c + k_a\bar{w}}\right] \tag{3.12}$$

$$c \equiv \frac{d_1 k_a}{d_2 k_{ca}}\frac{k_{mc}\bar{w}}{k_c + k_a\bar{w}} > 0 \tag{3.13}$$

Thus the solutions for $\bar{x}_2$ are:

$$\bar{x}_2 \quad = \quad \frac{1}{2}\left[-b(\bar{w}) \pm \sqrt{b^2(\bar{w}) + 4c(\bar{w})}\right]$$

Since $c > 0$, the solutions are always real and only the positive sign of the square root leads to a nonnegative solution. Thus the fixed point is unique. This last equation with the choice of a positive sign, together with (3.5) and (3.8) complete the proof. □

Note that all the entries of the fixed point in closed loop are parameterized only by the exogenous input w.

Interconnection of systems $\mathcal{P}_1 - \mathcal{K}_1$ and $\mathcal{P}_2 - \mathcal{K}_2$

Let x_j^i denote the j-th entry of the state vector in the i-th system. From (3.11):

$$f_i(w_i) \quad \equiv \quad \frac{1}{2}\left[-b_i(\bar{w}_i) + \sqrt{b_i^2(\bar{w}_i) + 4c_i(\bar{w}_i)}\right] \quad = \quad \bar{x}_2^i$$

For readability the definitions of the constants and variables in (3.11) are defined next:

$$\begin{aligned}
b_i(w_i) &= \gamma_{1i} - k_{cai}^{-1}\delta(w_i) \\
c_i(w_i) &= \gamma_{3i}\delta(w_i) > 0 \\
\gamma_{1i} &= \frac{1}{k_{cai}d_{2i}}[k_{ai}d_{1i} + k_{mni}k_{ri}k_{cni}] > 0 \\
\gamma_{3i} &= \frac{d_{1i}}{k_{ai}d_{2i}} > 0 \\
d_{1i} &= k_n(k_{cni} + k_{mri}) > 0 \\
d_{2i} &= k_{ri}k_{cni} + k_{rbi}(k_{mri} + k_{cni}) > 0 \\
\delta(w_i) &= k_{ai}k_{mci}\frac{w_i}{k_{ci} + k_{ai}w_i} \geq 0
\end{aligned}$$

Recall the unitary positive feedback of $P_1 - K_1$ and $P_2 - K_2$ (see Figure 3.2 on page 23) is defined by:

$$f_1(w_1) = \bar{x}_2^1 = w_2 \qquad f_2(w_2) = \bar{x}_2^2 = w_1$$

and the appropriate constants for each system are defined in Table 3.1. Closing the loop:

$$f_2 \circ f_1(w_1) \quad = \quad w_1 \tag{3.14}$$

With the nominal parameters, the solution for w_1 to (3.14) is:

$$w_1 = 0., w_1 = 0.393609, w_1 = 5161.58$$

In Figure 3.6 the function $f_2 \circ f_1(w_1)$ is shown with nominal parameters. In Figure 3.7 and 3.8 the solutions of $f_2 \circ f_1(w_1) - w_1 = 0$ are presented.

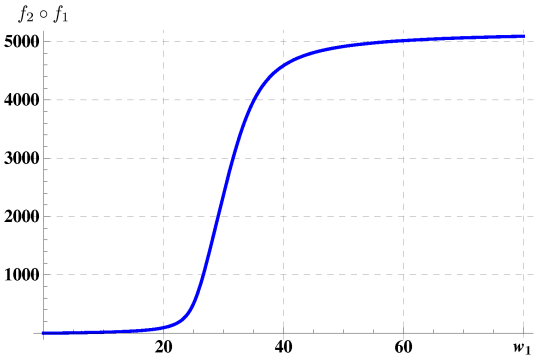

Figure 3.6: $f_2 \circ f_1$ with the nominal parameters

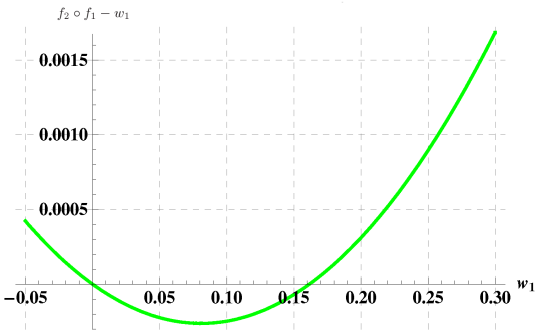

Figure 3.7: $f_2 \circ f_1 - w_1 = 0$ Detail for $w_1 < 1$

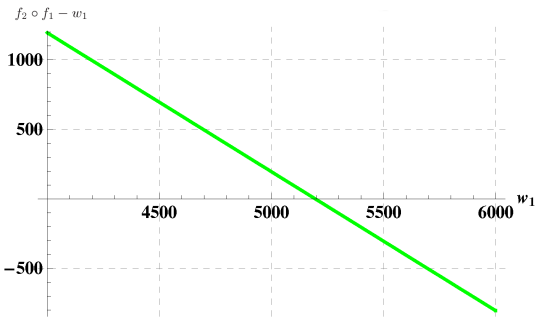

Figure 3.8: $f_2 \circ f_1 - w_1 = 0$ Detail for w_1 around the saturation of $f_2 \circ f_1$

Note from (3.14) that all the fixed points can be parameterized by w_1. i.e., the eight coordinates of the fixed point can be parameterized by only one coordinate. In Chapter 4, the bistability properties of the network will be explored.

3.1.3 Methodology summary

A summary of the procedure followed to identify the structure of the network is presented next.

S.1 Obtain the incidence graph with the matrix $\mathcal{L}$ (See 3.2)

S.2 Reorder the labeling of the nodes in order to reduce the bandwidth

S.3 Reorder the labeling so biochemical meaning is preserved (heuristic)

S.4 Identify the subsystems present as the blocks in the main diagonal and the interconnection signals as the off-diagonal terms

S.5 Analyze the (open loop) identified subsystems

S.6 Generate the block structure of the network

3.2 Intrinsic Apoptosis Pathway

The reactions of this pathway are presented in Section 2.3.3 and the mathematical model, in Appendix B.

3.2.1 Plant-Controller Scheme in the Intrinsic Apoptosis Pathway

Following the methodology presented in Section 3.1.3, the analysis of the model of the INAP is as follows:

S.1-4 The reduction of the bandwidth and the identification of the subsystems and interconnection signals are shown in Figure 3.9.

S.5 Structure identification. Let

$$\mathcal{P}_1 \quad : \quad \begin{cases} \dot{[C_{9a}]} &= -k_{54}[C_{9a}] - k_6[C_{3a}][C_{9a}] + u_{P_1-P_1} + u_{K_1} + u_1 \\ \dot{[C_{9P}]} &= -k_{53}[C_{9P}] + k_6[C_{3a}][C_{9a}] - u_{P_1-P_1} \end{cases}$$

$$\mathcal{P}_2 \quad : \quad \begin{cases} \dot{[C_3]} = & -(k_1 + k_5[C_{9a}] + k_7[C_{9P}] + k_8[C_{3a}])[C_3] + k_2 \\ \dot{[C_{3a}]} = & (k_5[C_{9a}] + k_7[C_{9P}] + k_8[C_{3a}])\,[C_3] - k_{55}[C_{3a}] + u_{K_2} \end{cases}$$

Claim 3.5. *The regulators of $\mathcal{P}_1$ and $\mathcal{P}_2$ are proportional derivative controllers.*

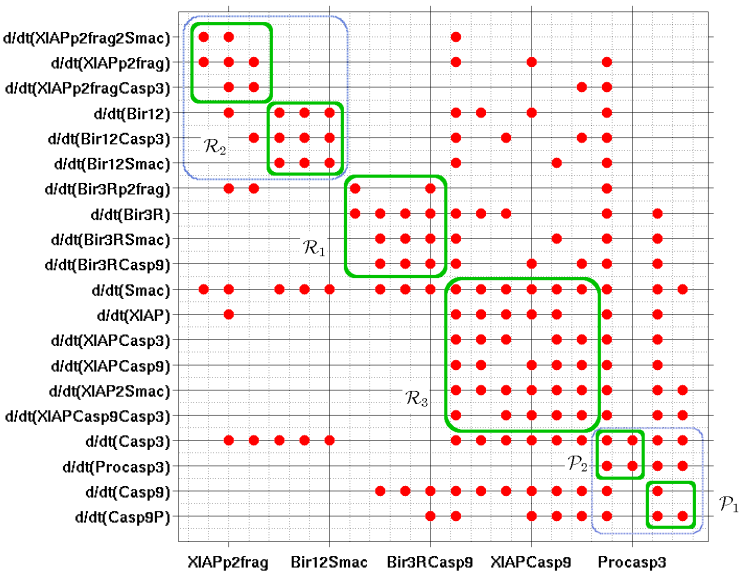

Figure 3.9: Sparse graph of the INAP model

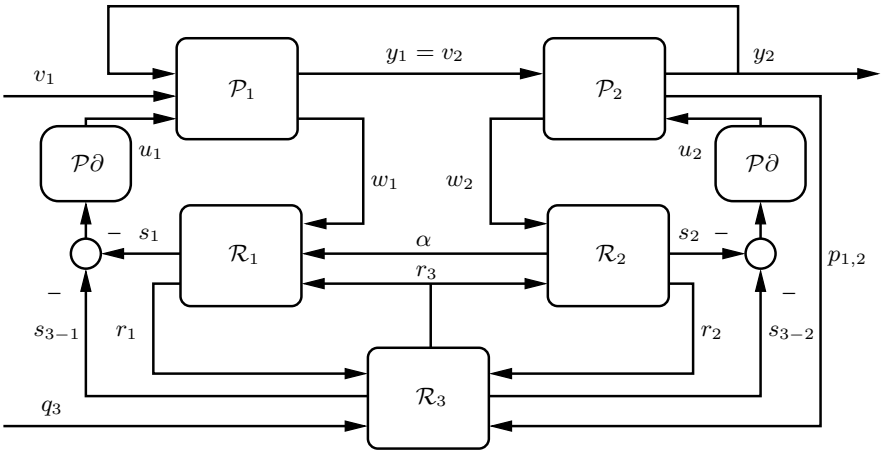

Figure 3.10: Block diagram representation for the INAP

The proof of Claim 3.5 is presented in Appendix C where is also stated that the error signals are:

$$\begin{aligned}\mathbf{e}_1 &= ([XIAP : C_{3a} : C_{9a}], [XIAP : C_{9a}], [Bir3R : C_{9a}]) \\ \mathbf{e}_2 &= ([XIAP : C_{3a} : C_{9a}], [XIAPp2frag : C_3], [XIAP : C_{9a}], [Bir12 : C_{3a}])\end{aligned}$$

S.6 The block diagram of the network is shown in Figure 3.10.

The definition of the interconnection signals is:

$$\begin{aligned}v_1 &= u_{Apoptosome} \\ y_1 &= ([C_{9a}], [C_{9P}])^T \\ w_1 &= [C_{9a}] \\ s_1 &= [Bir3R : C_{9a}] \\ s_{3-1} &= \begin{pmatrix}[XIAP : C_{9a}] \\ [XIAP : C_{9a}C_3]\end{pmatrix} \\ r_1 &= \begin{pmatrix}[Bir3R] \\ [Bir3Rp2frag] \\ [Bir3R : Smac] \\ [Bir3R : C_{9a}]\end{pmatrix} \\ \alpha &= \begin{pmatrix}[XIAPp2frag] \\ [XIAPp2frag : C_3]\end{pmatrix} \\ p_{1,2} &= \begin{pmatrix}[C_{3a}] \\ [C_{9a}] \\ [C_{9P}]\end{pmatrix}\end{aligned} \qquad \begin{aligned}y_2 &= [C_{3a}] \\ w_2 &= [C_{3a}] \\ s_2 &= \begin{pmatrix}[XIAPp2frag : C_3] \\ [Bir12 : C_{3a}]\end{pmatrix} \\ s_{3-2} &= \begin{pmatrix}[XIAP : C_{3a}] \\ [XIAP : C_{9a} : C_3]\end{pmatrix} \\ r_2 &= \begin{pmatrix}[Bir12] \\ [Bir12 : C_{3a}] \\ [Bir12 : Smac] \\ [XIAPp2frag : Smac] \\ [XIAPp2frag] \\ [XIAPp2frag : C_3]\end{pmatrix} \\ q_3 &= u_{Smac}\end{aligned}$$

3.2.2 Steady State Analysis

As can be seen from Appendix B, the complexity of the mathematical model makes it difficult to be analyzed. Moreover the system does not have any special characteristic with the nominal parameters, but reproducing the triggering of Intrinsic Apoptosis Mechanism. However, the basic interaction of caspases will be analyzed in order to provide a point of comparison with the EXAP. In the following sections, the analysis of the subsystems chosen as plants will be performed.

Caspase 9

Let $x = ([C_{9a}], [C_{9P}])^T$ and $w = [C_{3a}]$, then

$$\begin{aligned}\dot{x_1} &= -(k_{54}k_6w)x_1 - k_{53}x_2 + u_{K_1} + u_1 + u_{P_1-P_1} \\ \dot{x_2} &= -k_{53}x_2 + k_6wx_1 - u_{P_1-P_1}\end{aligned}$$

Fixed point

$$\begin{aligned}\bar{x}_1 &= \frac{\bar{u}_{P_1} + \bar{u}_{K1} + \bar{u}_1}{\bar{w}k_6 + k_{54}} \\ \bar{x}_2 &= \frac{k_6\bar{w}(\bar{u}_{K1} + \bar{u}_1) - k_{54}\bar{u}_{P_1}}{k_{53}(k_6\bar{w} + k_{54})}\end{aligned}$$

The equilibria loci is plotted in Figure 3.4 with defining $\alpha = (\bar{u}_{P1}+\bar{u}_{K_1}+\bar{u}_1)/k_{54}$, $\beta = (\bar{u}_{K_1} + \bar{u}_1)/k_{53}$, $\gamma = -\bar{u}_{P1}/k_{53}$.

Error variables

Let $n_1 = x_1 - \bar{x}_1$, $n_2 = x_2 - \bar{x}_2$. The deviation dynamics are:

$$\begin{pmatrix}\dot{n}_1 \\ \dot{n}_2\end{pmatrix} = \begin{pmatrix}-(k_{54} + k_6 w) & 0 \\ k_6 w & -k_{53}\end{pmatrix}\begin{pmatrix}n_1 \\ n_2\end{pmatrix}$$

Note that this system is the same as the one presented in Claim 3.1, hence this system is linear and stable, regarding w as a parameter.

Caspase 3

Let $\mathbf{z} = ([C_3], [C_{3a}])^T$ and $\mathbf{v} = ([C_{9a}], [C_{9P}])^T$.

$$\begin{aligned}\dot{z_1} &= -(k_1 - k_5 v_1 - k_7 v_2 - k_8 z_2)z_1 + k_2 \\ \dot{z_2} &= (k_5 v_1 + k_7 v_2 + k_8 z_2)\, z_1 - k_{55} z_2 + u_{K_2}\end{aligned} \tag{3.15}$$

Fixed points

The fixed point of (3.15) is:

$$\begin{aligned}\bar{z}_1 &= \frac{k_{55}\bar{z}_2 - u_{K_2}}{\theta + k_8\bar{z}_2} \\ \bar{z}_2 &= \frac{1}{2}\left(-\mu + \sqrt{\mu^2 + \frac{4}{k_8 k_{55}}(k_2\theta + \bar{u}_{K_2}[k_1 + \theta])}\right)\end{aligned}$$

where:

$$\begin{aligned}\theta &= k_5\bar{v_1} + k_7\bar{v_2} \\ \mu &= \frac{1}{k_8}(k_1 + \theta) - \frac{1}{k_{55}}(k_2 + \bar{u}_{K_2})\end{aligned}$$

Note that there is a selection of parameters that give a positive fixed point. Note also, that this positive fixed point is unique.

Without the exogenous inputs to the system (*cyt-c* and the formation of the Apoptosome) and the nominal parameters the only fixed point has all the entries set to zero except for those corresponding to Caspase 3 and IAP, whose numerical values are 0.1282 and 0.0603, respectively.

3.3 Conclusions

It has been shown that the formation, dissociation and degradation of a reactant can be represented as a regulating proportional-derivative action in a network of reactions. This effect is present in both pathways in the networks presented. It is a well known fact that inappropriate selection of the controller's parameters may lead to a undesired closed-loop behavior. In this regard, the selection of parameters is fundamental to guarantee the nominal performance of the network. In this work, the parameters are not freely eligible, but they are characteristic of the chemicals taking part in the network. This fact shows the level of organization present in living beings: the chemicals are not only being created and degraded in the appropriate quantity, but the way they do it, influence and regulate other compounds in the network. Note that the proportional gain of the controller is the rate of degradation of the so-called 'error signal'.

The conclusions obtained along the chapter can be summarized as follows:

EXAP

- Despite the complexity of the model, it can be regarded as a simple interconnection of four two-states systems
- The model can be analyzed as a decentralized control system
- Each of the four subsystems are open-loop stable, assuming the positiveness of the constants
- Each of the four subsystems has only one (stable) fixed point
- Both regulators present in the interconnected system can be viewed as PD controllers

INAP

- The mathematical model of this pathway does not seem to present any peculiar dynamical characteristic, but reproduces accurately the evolution of the experimentally measured concentrations in time
- The system can be thought of an *almost* decentralized controlled system
- The eight regulatory mechanisms can be represented as PD controllers

In the following two chapters analysis will be performed in order to determine limits on the parameters such that the characteristic properties of the network are preserved.

Chapter 4

Bistability Analysis

In this chapter a brief overview of three different approaches to characterize the multistability are presented. The model analyzed is the EXAP, since it is the only one which presents two stable fixed points with the nominal parameters. Although this model seems to present a bistable property, no global conclusion can be achieved. Nevertheless the conclusions achieved allow to determine which are the possible scenarios that the network may present and which are the parameters of the system that alter the bistable structure more significantly.

4.1 Introduction

In general, a variation on the parameters in a dynamical system can modify its equilibria set, drastically changing the qualitative behavior of the system. This phenomenon, called bifurcation, can lead to a change of the stability characteristic of a point of interest, hence destroying the usefulness of the system, in some cases. An interesting question that arises is to determine the biggest deviation of the nominal parameters such that the qualitative behavior of the network is preserved. Several approaches have been developed to answer these questions, exploiting different dynamical and structural properties.

In the next sections, the monotonicity and the graph of the reaction network are analyzed for the EXAP model, but no conclusions are achieved. Therefore, a classical bifurcation analysis is performed, resulting in the identification of the possible local behaviors of the model with variation of only one parameter at a time.

4.2 Monotonicity

A real function $y(x) : Re \rightarrow Re$ is said to be monotonic increasing if for every $\varepsilon > 0$

$$y(x + \varepsilon) - y(x) > 0$$

and strong monotonic increasing if the inequality is strict. The same definitions can be made for a monotonic decreasing function, with the appropriate selection of the inequality sign. The main qualitative property of this kind of functions is that they preserve order.

When the function $y(x)$ is not scalar, the symbols "$<$" and "$>$" are no longer naturally defined. Nevertheless, a partial order in a general Banach space ($\mathbf{B}$) can be defined given that two elements $x_1, x_2 \in \mathbf{B}$ satisfy the relation $x_1 - x_2 \in K$, where K is a nonempty, pointed cone.

With this in mind, a dynamical system $\phi : K \times X \subset \mathbf{B} \rightarrow X$ is monotone if and only if:

$$x_1 \geq x_2 \implies \phi(t, x_1) \geq \phi(t, x_2)$$

That is to say that the order imposed by the selection of the initial conditions is preserved in the trajectory of the system in a given time t. It can be shown that this special property can lead to very restricted trajectories of the state and strong conclusions about stability, under some assumptions. For instance, no chaotic or periodic trajectories exist in a monotone system (Hirsch and Smith, 2005).

In (Angeli and Sontag, 2003a) the extension of the concept of a monotone system with inputs and outputs is defined, via the assignation of an order in the space of inputs and outputs. Let u denote the input of the system and $h(x)$ represent the output, then a system is input-output monotone if and only if:

$$u_1 \geq u_2, x_1 \geq x_2 \implies h(t, x_1, u_1) \geq h(t, x_2, u_2)$$

It can be shown that the interconnection of two monotone systems under positive feedback is monotone, thus making the theory suitable for analyzing large scale, decentralized systems.

An easy way to determine whether or not a system is monotone is to analyze the incidence graph of the system. It is obtained as follows (Angeli et al., 2004): for a system with n states, the graph has $n + 2$ nodes (the extra nodes are the input and the output of the system). An arrow is drawn from a node x_j to a node x_i $\forall i$ such that $j \neq i$, if x_j affects directly the rate of change of x_i. Also a sign is assigned to this arrow: $+$ if the effect of x_j of positive and $-$ if its negative. The sign of a path is the product of these signs along a closed trajectory in the graph.

In (Angeli and Sontag, 2003b) it is stated that a system which admits an incidence graph is monotone with respect to some orthants for the states, the input and the output if and only if its graph does not contain any negative cycles. Moreover, under some stability and assumptions, two monotone systems can be interconnected and the set of fixed points can be easily determined and characterized. This conclusions can be guaranteed in the whole state space, thus obtaining a sound global characterization of the interconnected system.

In the case of the EXAP, the incidence graph is shown in Figure 4.1, where the separation of the system introduced in Section 3.1.2 is presented.

Unfortunately the model of the EXAP is not monotone -since the sign for some of the paths are negative: the path w_1, C_8, C_{8a}, w_1, for example- and no conclusion on

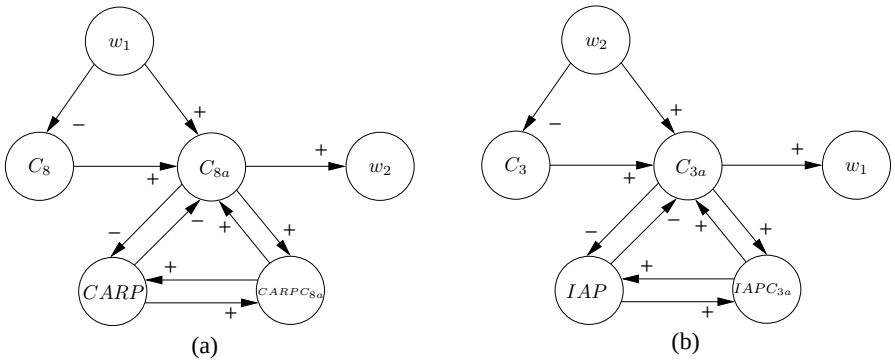

Figure 4.1: Incidence graph for the EXAP

the multistable properties of this system can be made using this theory.

4.3 Chemical Reaction Network Theory

The Chemical Reaction Network Theory based on the work of Horn, Jackson and Feinberg (Feinberg, 1979, for example) was developed to predict the behavior of a chemical reaction network based on its reaction diagram. Despite strong nonlinearity inherent in the mathematical model of a reaction network, the evolution in time of the concentration of the reactants and products is very restricted (the trajectories of the concentration in time can only belong to a subspace called the 'compatibility class' determined by the 'reaction vectors of the network', which represent the direction in which a concentration is being modified). Moreover, under some strong assumptions on the incidence graph of the network, the evaluation of a sole index can determine the way the phase portrait looks and thus the qualitative trajectories of the concentrations can be determined. This index is called the deficiency of the network.

A basic assumption for this theory to apply, is a weak reversibility property of the incidence graph of the network: if there exist a directed path going from node x_i to node x_j, there must exist another directed path going from x_j to x_i, directly or indirectly through other nodes. The main drawback of this methodology is that this requirement is too restrictive.

In the case of the EXAP, the weak reversibility property is not complied by the model (see from Figure 4.1(a) that there exists a path joining C_8 to C_{8a}, but there is no path in the opposite direction). Thus no conclusion can be made using this theory.

4.4 The EXAP model as a general dynamical system

The fact that the system is not monotone or that the graph is not weakly reversible, does not mean the system is not globally multistable. It only means that this system does not have the mentioned properties: exhaustive simulations changing the initial

concentration show that the only behavior of the system with the nominal parameters is the convergence to either of the stable fixed points (data not shown), but no formal proof has been done in this regard. In the present section the characterization of the bistability properties of the system will be performed via a classical bifurcation analysis with the variation of one parameter at a time. This analysis intends to show the possible behaviors of the model and to determine the structural robustness of the (local) bistability of the system to variation in parameters.

In (Eissing, 2007) a nontraditional bifurcation analysis is performed via the Monte Carlo approach, since the traditional analysis considering the variation of all parameters at a time is very demanding in computational terms. Here, a parameter is perturbed off the nominal value in order to explore the possible behaviors the systems can have. A structural robustness index will be evaluated in terms of keeping the qualitative properties of the equilibria set: two stable and one unstable fixed points.

For doing this, consider the equation (3.14 on page 30) presented below, for readability. Recall that the allocation of the eight coordinates of the fixed points is parameterized by only one of them: w_1.

$$f_2 \circ f_1(w_1) \quad = \quad w_1 \tag{4.1}$$

where (defined in 3.1.2),

$$\begin{aligned}
f_i(w_i) &= \frac{1}{2}\left[-b_i(w_i) + \sqrt{b_i^2(w_i) + 4c_i(w_i)}\right] \\
b_i(w_i) &= \gamma_{1i} - k_{cai}^{-1}\delta(w_i) \\
c_i(w_i) &= \gamma_{3i}\delta(w_i) > 0 \\
\gamma_{1i} &= \frac{1}{k_{cai}d_{2i}}[k_{ai}d_{1i} + k_{mni}k_{ri}k_{cni}] > 0 \\
\gamma_{3i} &= \frac{d_{1i}}{k_{ai}d_{2i}} > 0 \\
d_{1i} &= k_n(k_{cni} + k_{mri}) > 0 \\
d_{2i} &= k_{ri}k_{cni} + k_{rbi}(k_{mri} + k_{cni}) > 0 \\
\delta(w_i) &= k_{ai}k_{mci}\frac{w_i}{k_{ci} + k_{ai}w_i} \geq 0
\end{aligned}$$

The definition of the parameters is presented in Table 3.1 on page 24.

Remark 4.1. *The solutions of $f_2 \circ f_1(w_1) = w_1$, which parameterize the fixed point, satisfy:*

- $w_1 = 0$ *is always a solution.*

This can be seen as follows:

$$\begin{aligned} f_i(0) &= \frac{1}{2}\left[-b_i(0) + \sqrt{b_i^2(0) + 4c_i(0)}\right] \\ &= \frac{1}{2}[-\gamma_{1i} + \gamma_{1i}] \\ f_i(0) &= 0 \end{aligned}$$

Hence, $f_2 \circ f_1(0) = 0$

- *In Figure 4.2 can be seen that* $w_1 \approx max(f_2 \circ f_1(w_1))$ *is a solution when the function* $f_2 \circ f_1(w_1)$ *saturates 'faster' than the line* w_1 *grows. As can be seen in Figure 4.2,* $f_2 \circ f_1(w_1)$ *has a sigmoidal characteristic and is monotonically increasing, thus the intersection with the unitary line will be near the ordinated pair* $(w_1, f_2 \circ f_1(w_1)) = (f_2 \circ f_1(w_1 \to \infty), f_2 \circ f_1(w_1 \to \infty))$.
  The maximum of the function $f_2 \circ f_1(w_1)$ *is obtained by noting:*

$$\begin{aligned} \lim_{w_i \to \infty} \delta(w_i) &= k_{ai} k_{mci} \frac{1}{0 + k_{ai}} \\ \lim_{w_i \to \infty} \delta(w_i) &= k_{mci} \end{aligned}$$

  Then

$$\lim_{w_1 \to \infty} f(w_1) = \frac{1}{2}\left[\frac{k_{mc1}}{k_{ca1}} - \gamma_{11} + \sqrt{\left(\gamma_{11} - \frac{k_{mc1}}{k_{ca1}}\right)^2 + 4\gamma_{31} k_{mc1}}\right]$$

  and in the closed loop, the composition of functions $f_2 \circ f_1(w_1 \to \infty)$ *has one real positive value. With the nominal parameters,* $f_2 \circ f_1(w_1 \to \infty) \approx 5161.58$*, the actual solution to (4.1).*

If no selection of parameters is made, the closed loop function (4.1) can be used to determine the set of parameters that lead to the existence of three solutions. Note that as the parameters vary the plot of (4.1) in Figure 4.2 will deform. See for example Figure 4.3, where only one parameter is varying. In a limit condition, the line and the sigmoid will be tangent. The tangency point w_1^+, satisfies (Alvarez, 2008):

C1 $f_2 \circ f_1(w_1^+) = w_1^+$, i.e., the line and the sigmoidal curve has to intersect each other

C2 $D_{w_1} f_2 \circ f_1(w_1)|_{w_1^+} = 1$, that is to say that beside finding a solution in w_1^+ the curves have to be tangent in this point.

The two conditions above, can be used to find all the bifurcation points as a function of the parameters. Nevertheless, the function (4.1) and $D_{w_1} f_2 \circ f_1(w_1)|_{w_1^+} = 1$ are too complicated to be treated analytically and no conclusion regarding bistable behaviour can be made, notwithstanding this equations has been used to give insight to the structure of this model. Note that finding the restriction of the parameters that lead

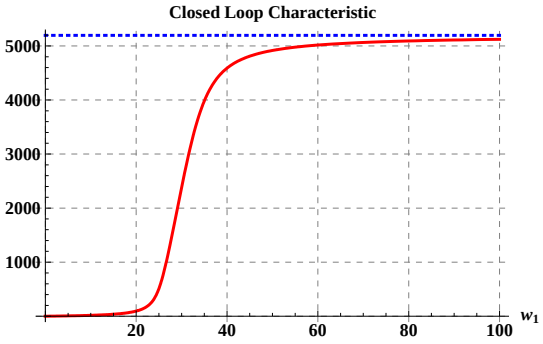

Figure 4.2: $f_2 \circ f_1$ with the nominal parameters

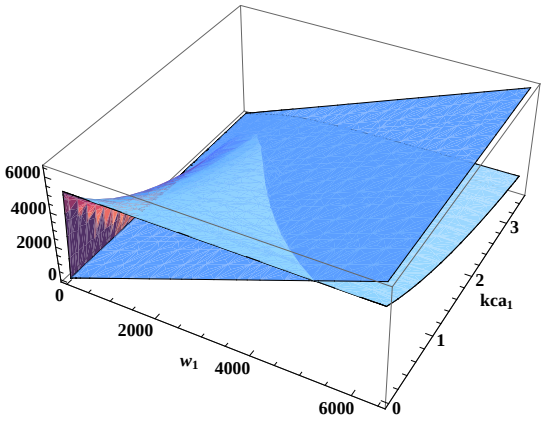

Figure 4.3: $f_2 \circ f_1$ with the variation of the parameter k_5 (k_{ca1})

to three fixed points does not guarantee that two of them will be stable and the other unstable, but a further analysis can be made.

Instead a bifurcation analysis is performed as follows:

i Compute the linearization of the model, as a function of the parameters and the fixed point

ii Choose a value for the chosen parameter and leave the value of the rest as nominal

iii Find all the fixed points of the model with this set of parameters

iv Evaluate the linearization in the fixed points found and the parameters and determine the stability property of each solution

v Then go to step ii until a desired parameter range has been explored

Following this procedure, the bifurcation diagrams are obtained. Although every parameter has an effect on the location of the fixed points, Figures 4.4 to 4.7 show some representative cases. Special care should be taken when reading the graphs since the w_1 axis is logarithmic for $w_1 > 1$ and linear for $w_1 \in [0, 1]$. The 'x' axis is the relative, absolute error of the value of the parameter respect to the nominal parameter in percent. In the bifurcation diagrams the red color will represent instability and the blue one, stability.

Table 4.1 shows the bounds of the parameters that preserve the bistability conditions.

4.5 Conclusions

In the present context, only a local characterization of the multistable properties of the EXAP model could be achieved, since it fails to comply some well-known properties that help to explain a global behavior, such as monotonicity. Nevertheless, the local bifurcation analysis performed, shows that multiple scenarios are possible, when a parameter is varied. The key for this procedure to apply is the capability of the system's fixed points to be parameterized by w_1, because the qualitative behavior of the system can be analyzed in a 2D plot. Recall that w_1 is the $[C3_a]$.

From Figure 4.4, it can be seen that a large enough variation in the positive direction of the parameter k_2 can make the 'life' fixed point unstable and possibly leading to the death of the cell.

Figures 4.6 and 4.7 are presented to show that in general three scenarios are possible: one fixed point with low level of w_1, a bistable switch and one fixed point with high level of w_1.

An interesting remark is that in all cases, the nominal parameter is close to a bifurcation point. This fact implies that the structural stability is very fragile, since a small variation of the parameter can destroy the structural property of the network. It is interesting that the structural bistability is more sensible to the parameters that represent the zero order reactions and to the mutual activation of caspases (k_{m10},k_{m3},k_{m9},k_1,k_2,k_{m11}).

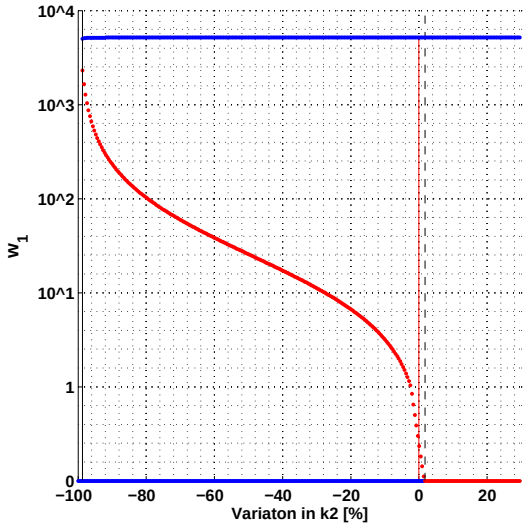

Figure 4.4: Bifurcation diagram for parameter k_2

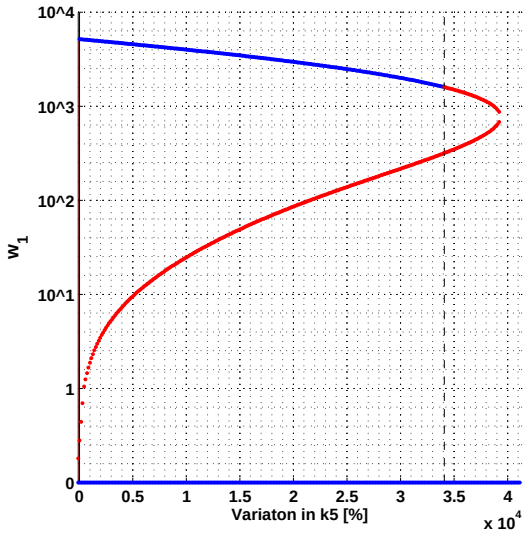

Figure 4.5: Bifurcation diagram for parameter k_5

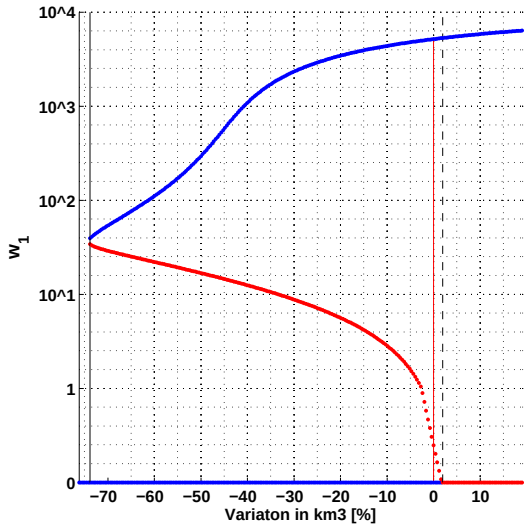

Figure 4.6: Bifurcation diagram for parameter k_{m3}

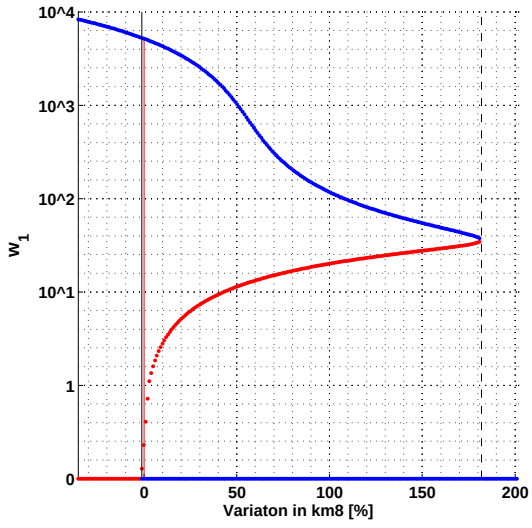

Figure 4.7: Bifurcation diagram for parameter k_{m8}

Table 4.1: Limits on the the parameters to present bistability.
This table is sorted according to the total percent of allowed variation in the parameter, such that bistability is preserved (Superior Bound - Inferior Bound).
* = A negative value of the parameter still leads to a bistable scenario, thus is not considered in the ranking.
* * = A variation larger than 100 000[%] still leads to a bistable scenario and is ignored in the ranking.

	Nominal Parameter	Inferior Bound [%]	Superior Bound [%]
k_{m10}	81.9	-64.29	1.79
k_{m3}	0.21	-73.81	1.98
k_{m9}	507.0	-90.14	1.85
k_2	0.00001	-98.70	1.65
k_1	0.000058	-99.43	1.65
k_{m11}	0.21	-100.00	1.97
k_{m8}	464.0	-1.50	181.90
k_3	0.0005	-1.50	218.00
k_7	0.0173	-1.50	286.90
k_{m12}	40.0	-1.65	1145.00
k_9	0.0039	-1.53	11430.00
k_6	0.0058	-19.54	23880.00
k_5	0.0058	-17.24	34110.00
k_{10}	0.0039	-1.50	38330.00
k_{12}	0.001	*	1.87
k_8	0.0116	*	1.72
k_4	0.0003	*	**
k_{13}	0.0116	-1.50	**
k_{11}	0.0005	-1.50	**

When interpreting the diagrams special caution has to be taken. The presented plots show a bifurcation diagram with the variation of only one parameter at a time. When more than one parameter are varied at a time, the resulting diagrams would look very different. Note also that the results presented here are only local and by no means characterize the global behavior of the system, hence other strange attractors might exist.

Chapter 5

Robustness Analysis

Introduction

Cellular reaction mechanisms are robust to noise and parameter uncertainty. A clear example is the apoptosis process which is the mechanism the cell uses to decide whether it continues living or not. In the present context, it is strongly dependent on the structure of the pathway itself, and, surprisingly, solely on a couple of kinetic parameters. In order to determine which parameters are more important, the structured singular value analysis (SSV) is applied to the linearization of the model about the "life" fixed point.

5.1 Introduction to the Structural Singular Value

5.1.1 Robust Stability

Once the structure of a model is attained, the main issue is the right choice of the parameters that characterize the reactions in the pathway, so the model accurately represents the observed phenomena. Given the variability of parameters among the cells, a set of parameters that preserve the desired behavior is a better characterization of the model. In this context, an analysis of the robustness of the stability and a performance index of the model can retrieve such sets.

In the case of both apoptosis pathways, one approach is to determine which is the smallest perturbation in a parameter for which the stability of a fixed point is preserved. The fixed point considered will be the 'life' steady state. The destruction of the stability of this point will mean the incapability of the cell to maintain itself alive, resulting, -presumably- in a disease as stated in Chapter 1.

The theory is well established for linear systems via the computing of the Structural Singular Value (SSV) μ of a linear system. In the present case, a perturbation of each parameter will be considered with the aim of identifying the most important reactions in terms of stability preservation, i.e., the parameters that can have the smallest variation in order to preserve the stability of the analyzed fixed point.

The whole theory of the SSV relies upon the Small Gain Theorem , which states the necessary and sufficient conditions for a interconnection of n interconnected $\mathcal{L}_{pe}$ stable systems to be $\mathcal{L}_{pe}$ stable.

Theorem 1. *Given the interconnection shown in Figure 5.1 with $M(s) \in C^{pxq}$, $M(s) \in \mathcal{L}_p$ and $\gamma > 0$. The interconnected system is well-posed and internally stable for all $\Delta(s) \in \mathcal{L}_p$ with*

a) $||\Delta||_p \leq \gamma^{-1}$ if and only if $||M(s)||_p < \gamma$

b) $||\Delta||_p < \gamma^{-1}$ if and only if $||M(s)||_p \leq \gamma$

The proof of the Theorem can be found in (Khalil, 2001) or (Zhou et al., 1996), for example.

In Figure 5.1 the perturbation matrix is represented by the the $\Delta(s)$ block and the system by the $M(s)$ block. Regarding the Theorem above it is possible to know the maximum $\mathcal{L}_{pe}$ of the perturbation such that the interconnection preserves the property of both blocks. For instance, let this maximum norm be $||\Delta||_\infty = \beta^{-1}$, then the maximum norm such that the interconnection preserves the stability is:

$$\beta = ||M||_\infty = sup_{s \in C_+} \overline{\sigma}(M(s)) \tag{5.1}$$

As can be seen, Theorem 1 is defined for linear systems so in order to apply it to the current problem, the linearization of the Apoptosis model has to be taken into account. In (Dunne, 2008) it is shown that about the 'life' fixed point, the EXAP, behavior is almost linear, and a good estimate of the actual nonlinear robustness can be obtained at least very close to the linearization point. Let this linearization be denoted by

$$\begin{aligned} \dot{x} &= Ax + Bu \\ y &= Cx, \end{aligned} \tag{5.2}$$

and assume the perturbed system is $A_p = A + A_i$, so the transfer function from $U(s)$ to $X(s)$ can be rewritten as in Figure 5.2, as stated in (Shoemaker and Doyle, 2008). Via a Linear Fractional Transformation , as shown in Figure (5.3), the interconnection studied in the Small Gain Theorem can be achieved.

Once this interconnection is obtained, the transfer function from $U(s)$ to $X_i(s)$ (where the subindex i denotes the signal regarding the perturbation A_i) is:

$$\begin{pmatrix} y_p \\ x_i \end{pmatrix} = \underbrace{\begin{pmatrix} P_{11} & P_{12} \\ P_{21} & P_{22} \end{pmatrix}}_{\mathbf{P}} \begin{pmatrix} u_p \\ u \end{pmatrix} \tag{5.3}$$

Regarding Figure 5.3-b, the Upper Linear Fractional Transformation of the system is:

$$x_i = \left(P_{22} + P_{21}\Delta(I - P_{11}\Delta)^{-1}P_{12}\right) u_i \tag{5.4}$$

Since $P_{22} : U \rightarrow X_i$ is a $\mathcal{L}_p$ stable map, the only source or instability in (5.4) is $P_{21}\Delta(I - P_{11}\Delta)^{-1}P_{12}$. The stability of that transfer function is guaranteed by the

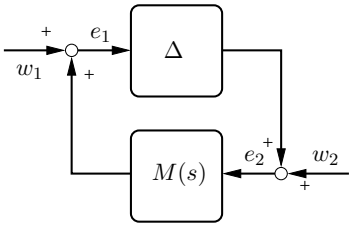

Figure 5.1: Positive feedback interconnection of two systems

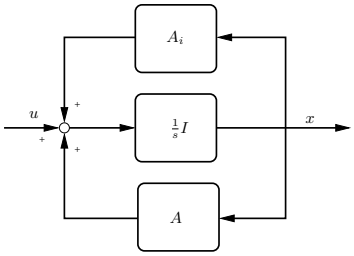

Figure 5.2: Perturbed system, where A denotes the nominal system and A_i, the perturbation to the nominal system.

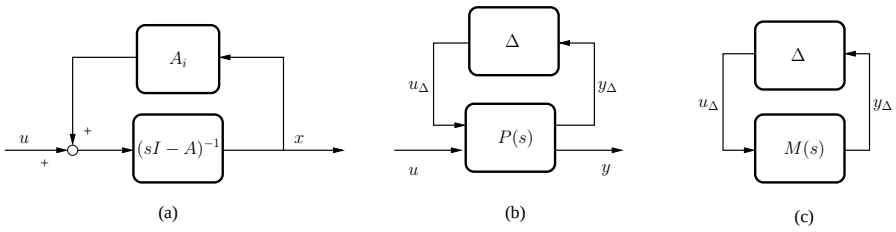

Figure 5.3: Rewriting the system via LFT (a) A perturbed system as a closed loop interconnection. (b) The interconnection of the system in the general control formulation. (c) Separating the effect of the perturbation on the system.

multivariable Nyquist stability criterion:

$$det(I - M\Delta) \neq 0$$

where $M \equiv P_{11}$. In order to determine the size of the maximum perturbation the system can endure and maintain stability, the definition of the SSV μ (Skogestad and Postlethwaite, 1996) seems natural:

$$\mu_{\Delta}^{-1}(M(s)) \equiv min\{k_{dj}|det(I - M\Delta(s, k_{dj})) = 0\} \tag{5.5}$$

The meaning of the subindex j will become clear in the next sections.

If the system is stable, the meaning of k_{dj} is the smallest gain that push the closed loop poles into the imaginary axis. In case the system were not stable, the gain k_{dj} is the smallest gain that brings the system to stability. In a general context, it is no possible to have the actual value of μ. Instead bounds are computed in order to estimate the size of the perturbation ($\rho(M) \leq \mu_{\Delta}(M) \leq \overline{\sigma}(M)$). Even tighter bounds can be computed regarding the structure of the perturbation and the system itself, when the information is available.

5.1.2 Robust Performance

In general, not only robust stability has to be maintained, but also a "good" performance is desirable despite the presence of a perturbation. In the context of the case of study a good performance means that the mechanism of Apoptosis is triggered in the expected way even if an actual parameter is not nominal. In order to establish a meaningful comparison among the difference of the nominal response and the perturbed response, a weight function ($W_e(s)$) has to be designed such the magnitude of the error between the responses is amplified in a representative frequency interval.
In order to perform the analysis, (Shoemaker and Doyle, 2008) propose the interconnection in Figure 5.4, which can be rewritten in the general scheme shown in Figure 5.3-b with the output being z rather than x_i:

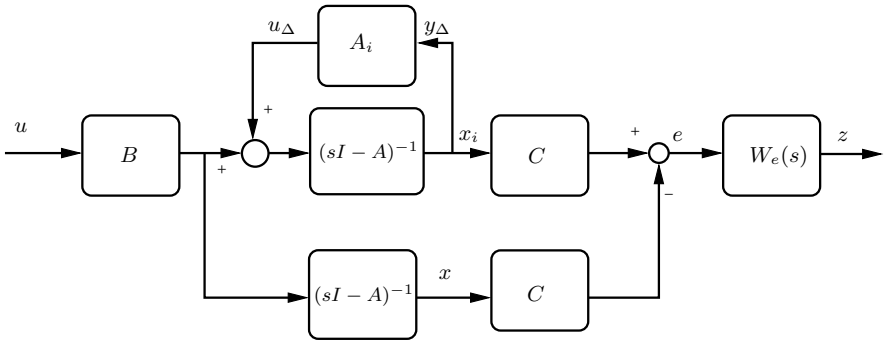

Figure 5.4: Performance assessment scheme

$$\begin{pmatrix} y_p \\ z \end{pmatrix} = \begin{pmatrix} (sI-A)^{-1} & (sI-A)^{-1}B \\ W_eC(sI-A)^{-1} & 0 \end{pmatrix} \begin{pmatrix} u_p \\ u \end{pmatrix}$$

The closed loop obtained via Upper Linear Fractional Transformation is:

$$\mathcal{F} = WeC(sI-A)^{-1}\Delta\left(I-(sI-A)^{-1}\Delta\right)^{-1}(sI-A)^{-1}B \quad (5.6)$$

Define $\beta \equiv ||F||_\infty$. The performance condition can be formulated as finding the smallest size of the perturbation such that the weighted norm of the error z is less or equal than 1, i.e., find k_{pi} such that:

$$||\Delta(s,k_{ij})||_\infty = \frac{1}{\beta} \quad (5.7)$$

Recalling $k_{ij} \in \Re$ and, both, (5.6) and (5.7), the performance condition can be expressed as:

$$\begin{aligned} ||\Delta(s,k_{ij})||_\infty||\mathcal{F}(s,k_{ij})||_\infty \leq 1 \\ ||\mathcal{F}(s,k_{ij})||_\infty \leq \beta \end{aligned} \quad (5.8)$$

Note that the value of k_{ij} is the supremum value for which the performance index is achieved with the proviso that the internal stability of the system.

5.2 Methodology

In order to determine the set of parameters which maintain the robust stability and performance of the system, a suitable construction of the perturbation has to be chosen. In this case, let one variation of parameter at a time and assume that the perturbation of each parameter is of the form: $k_{ij} = k_j + k_{dj}$, where the subindex i stands for perturbed parameter; d for the disturbing term and j is the defines the $j-$th entry of the parameter vector. In that case, the perturbed Jacobian is:

$$A_p = A + A_i(k_{dj}),$$

where $A_i(k_{dj})$ is obtained evaluating $A(\mathbf{k})$ in a vector whose $j-$th entry is k_{dj} and zero otherwise.

In section 5.1.2 has been shown that such a perturbation can be written in the form of (5.3 on page 48). Identifying the perturbation -in this case as $\Delta = A_i(k_{dj})$- from Figure (5.3), the general formulation (5.3) becomes:

$$\begin{pmatrix} y_\Delta \\ x_i \end{pmatrix} = \begin{pmatrix} (sI-A)^{-1} & (sI-A)^{-1} \\ (sI-A)^{-1} & (sI-A)^{-1} \end{pmatrix} \begin{pmatrix} u_\Delta \\ u \end{pmatrix}$$

Thus the Structured Singular Value (5.5) becomes:

$$\mu_\Delta^{-1}(M(s)) = min\{k_{dj}|det(I-(sI-A)^{-1}A_i(k_{dj}))=0\}$$

By construction, $A_i(k_{dj})$ is affine in k_{dj}, so this condition becomes:

$$\mu_{\Delta}^{-1}(M(s)) = min\{k_{dj}|det(I - k_{dj}(sI - A)^{-1}A_i) = 0\} \tag{5.9}$$

Recalling that k_{dj} is just a scalar, the actual solution can be computed by just solving:

$$det(I - k_{dj}(sI - A)^{-1}A_i = 0)$$

as a function of s. The actual values are computed in Matlab with the code listed in the Appendix D. Figure (5.5) shows the plot for the structured singular value for the parameter k_8 in the INAP, as an example.

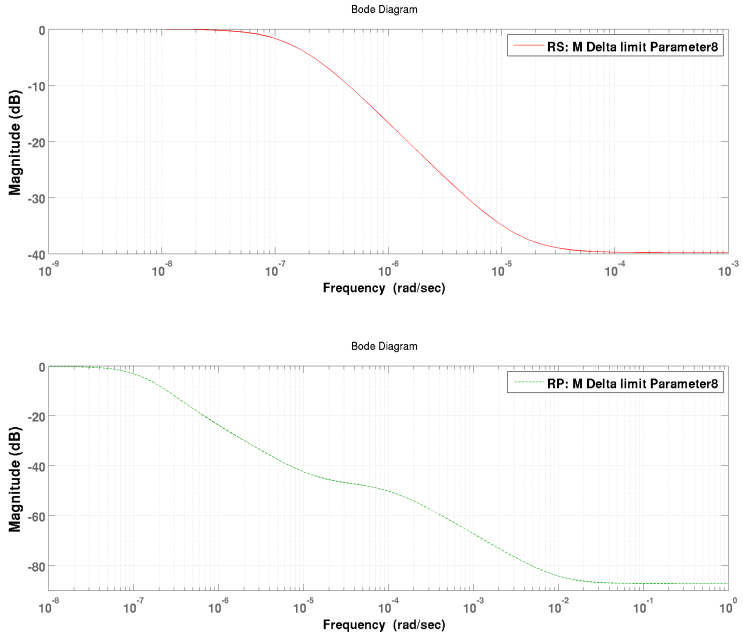

Figure 5.5: $||M||_{\infty}||\Delta||_{\infty}$ for k_8 in INAP

In order to achieve robust performance a weight function is defined (Skogestad and Postlethwaite, 1996):

$$W_e(s) \quad = \quad \frac{s/M + \omega_B^*}{s + \omega_B^* \alpha}$$

where $|W_e(i\omega)|^{-1}$ is equal to α in low frequencies and M in high frequencies. The asymptote crosses 1 at ω_B^*. In this case, the parameters of weight function has been

selected to increase the error in the resonance frequencies of the transfer function from u to z of Figure 5.4. With this selection, the weight function becomes:

$$W_e(s) \quad = \quad 5000\frac{0.1s + 0.001}{s + 0.0001}$$

Recalling the definition of the perturbation, the performance condition (5.8) becomes:

$$||k_{pi}A_i||_\infty ||k_{pi}W_eC(sI - A)^{-1}A_i\left(I - k_{pi}(sI - A)^{-1}A_iB\right)||_\infty \leq 1 \qquad (5.10)$$

which can be solved numerically for k_{ji} by the optimization of (5.10) assuming it is a convex property. The code is also available in the Appendix D, and Figure (5.5) shows the Bode magnitude plot for the previous condition on the limit value for k_8 as an example, in the INAP.

5.3 Results

5.3.1 Extrinsic Apoptosis Pathway

Table 5.1 shows the maximum perturbation allowed per parameter using the Structured Singular Value analysis. The allowed perturbations that keep performance and the maximal allowed variation computed as $pk_j = |100(k_{dj}/k_j)|$, where k_j is the nominal value of the parameter and k_{dj} is the disturbance computed by the analysis. The entries filled with '*' are not present in the Jacobian.

5.3.2 Intrinsic Apoptosis Pathway

Table 5.2 shows the maximum perturbation allowed per parameter using the Structured Singular Value analysis in order to maintain both the performance and the stability. The parameters that are not shown, are not present in the linearization of the system.

5.4 Conclusions

The analysis presented here computes the smallest variation of the parameters that leads to the linerization about the 'life' fixed point to preserve the stability and a performance index. Notwithstanding, the ranking of the reactions shown in Tables 5.1 and 5.2 is just qualitative, since no real behavior is considered. As an example, consider the parameter k_{m11} whose variation in order to preserve the stability of the 'life' fixed point is 8.04[%]; in Chapter 4 it is shown that only a variation of +1.83[%] can destroy the bistable scenario.

An interesting result is that in both cases, the parameters that are more sensible are present in the controllers identified in Chapter 3.

Table 5.1: Maximal Perturbation that maintain stability and performance in the INAP (μ^{-1})
$* =$ This parameter is not present in the linearization. Hence it does not have any effect in either the stability or performance.

Stability Parameter	[%]	Performance Parameter	[%]
k_{m8}	*	k_{m8}	*
k_{m9}	*	k_{m9}	*
k_{m10}	*	k_{m10}	*
k_{m12}	*	k_{m12}	*
k_{m11}	8.040	k_{m11}	0.028
k_{m3}	8.232	k_{m3}	0.028
k_7	98.229	k_3	1.130
k_{13}	143.129	k_{11}	1.131
k_3	3144.100	k_7	1.184
k_{11}	3149.500	k_{13}	2.140
k_8	8620.700	k_8	37.406
k_9	25641.000	k_1	38.861
k_{10}	25641.000	k_4	45.699
k_1	27431.000	k_5	82.911
k_5	49009.000	k_6	99.875
k_6	71135.500	k_2	227.195
k_{12}	100000.000	k_{10}	352.012
k_2	159099.700	k_9	381.867
k_4	958356.400	k_{12}	1367.300

Table 5.2: Maximal Perturbation that maintain stability and performance in the INAP (μ^{-1})

Performance Parameter	[%]	Stability Parameter	[%]
k_9	4.95E-004	k_9	0.54
k_{27}	5.43E-004	k_{52}	0.64
k_7	2.96E-003	k_{27}	0.64
k_5	4.46E-002	k_7	2.07
k_{17}	7.22E-002	k_{44}	3.14
k_{52}	0.15	k_{46}	7.06
k_8	0.43	k_{17}	48.61
k_{46}	4.85	k_8	206.87
k_{10}	5	k_{32}	722.39
k_{28}	5.48	k_{16}	722.41
k_{44}	7.25	k_{36}	948.05
k_{56}	43.32	k_{56}	2316.3
k_{58}	47.47	k_{64}	2762.49
k_{36}	272.69	k_{57}	2881.6
k_3	285.27	k_{60}	2881.6
k_{64}	286.16	k_{69}	2881.6
k_{53}	782.93	k_{58}	2889.21
k_{16}	1299.36	k_{10}	4361.01
k_{32}	1541.36	k_3	8620.69
k_1	1643.66	k_{63}	13700.01
k_{63}	1824.20	k_{62}	13913.23
k_{62}	2634.55	k_5	15124.77
k_{57}	7107.86	k_{70}	17183.75
k_{60}	7107.86	k_{59}	17223.83
k_{69}	7107.86	k_{53}	17241.38
k_{55}	10586.52	k_1	25641.03
k_{54}	11597.79	k_{28}	198812.75
k_{70}	12310.79	k_{67}	445158.8
k_{59}	27460.78	k_{68}	445303.21
k_{66}	29656.36	k_{66}	1181494.62
k_{61}	60572.97	k_{55}	4533930.48
k_{67}	86190.46	k_{54}	5447129.05
k_{68}	250201.31	k_{61}	12938952.5
k_{65}	1272955.6	k_{65}	94748295.29

Chapter 6

Conclusions

In the present work two different apoptosis pathways are presented and dynamically analyzed. Due to the complexity of the differential equations arising from the reaction networks, no structural conclusions could be achieved. However, the symmetry property of the Extrinsic Apoptosis Pathway model, allows a simplification of its dynamical analysis.

It is shown that a particular set of reactions can lead to a proportional derivative controlling action. A subsequent analysis of the topology of the studied networks, leads to the identification of a decentralized controller scheme. Regarding the impact the variation of each parameter exerts in the bistability, robustness and performance of the network, the most important reactions are identified. The analysis of the multistable properties of the Extrinsic Apoptosis Pathway shows that monostable and bistable behaviors are possible. When only one fixed point is stable, the switch from 'life' to 'death' is not possible. In fact, this monostable scenario can be easily reached by varying some parameters only by two percent, showing that the structural property of bistability is not robust. It is important to remark that the conclusions obtained from the bistability analysis are local and strange attractors might exist.

The robustness of the stability and performance for both apoptosis pathways was analyzed using the Structural Singular Value. This allowed to identify the most sensible parameters in the reaction network. A comparison among the three analysis performed is presented in Figure 6.1.

It is remarkable that the parameters k_{m10} and k_{m9} do not play any role in neither the robust stability analysis nor in the robust performance analysis, but they are one of the most important in the bifurcation analysis. In general, the results obtained with the robust stability analysis are bigger than those obtained with the bifurcation analysis. The reason for this is that the linearization is studied in the case of the former analysis and only local conclusions can be obtained.

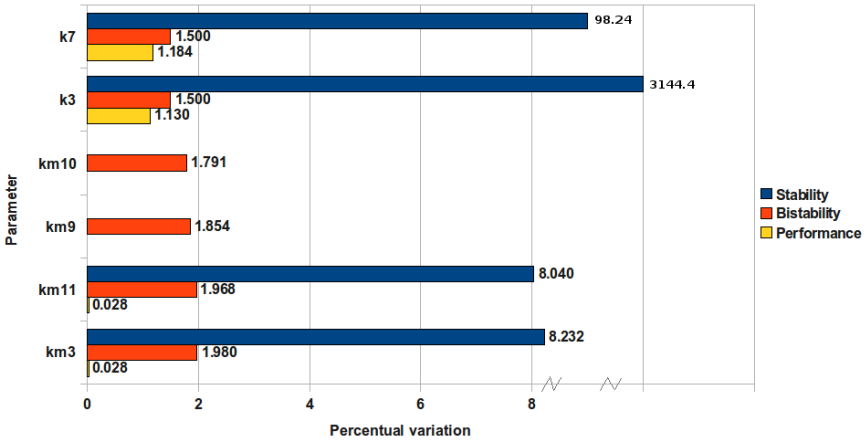

Figure 6.1: Comparison among the different analyses. When a bar is not present in a parameter, the variation in this parameter can be arbitrarily large and no effect will be observed on the property under consideration.

Appendix A

Reducing the Matrix Bandwith

Most of the contents present in this section are taken from (Diestel, 2000) and (Marti et al., 2001), where a novel algorithm, based on tabu search, for reducing the bandwidth of a matrix is presented and compared with the leading algorithms.

A graph is a a pair $G = (V, E)$ of sets satisfiying $E \subset [V]^2$, where $[V]^n$ denotes the power set of V up to n-tupels of elements. The elements of V are called the *vertices* of the graph G, the elements of E are its *edges*. $|G|$ denotes the *order of* G (number of vertices) and $||G||$, the number of edges. Two vertices u, v are adjacent if uv is an edge of G.

Let $f(v)$ be the label of vertex $v \in V$, where each vertex, has a different label. The bandwidth of a vertex v, $B(f(v))$, is the maximum of the differences between $f(v)$ and the labels of its adjacent vertices:

$$B_f(v) = \max\{|f(v) - f(u)|\forall u \in N(v)\}$$

where $|f(v) - f(u)|$ denotes the absolute value of $f(v) - f(u)$ and $N(v)$ is the set of vertices adjacent to v. The bandwidth of a graph G with respect to a labeling f is

$$B_f(G) = \max\{B_f(v)\forall v \in V\}.$$

Let $B(G)$ be the minimum $B_f(G)$ over all possible labelings f. The bandwidth reduction problem consists of finding a labeling f that minimizes $B_f(G)$. Let $l_{ij} \neq 0$ if $ij \in E$ and $\mathcal{L} = \{l_{ij}\}$ be the incidence matrix. Regarding this definitions, the bandwith reduction problem consists of finding a permutation of the rows and the columns that keeps all the non-zero elements of $\mathcal{L}$ in a band that is as close as possible to the main diagonal.

Several algorithms for solving the bandwidth problem has been developed since the late 1960's (see (Marti et al., 2001)). Being the most important:

1969 Reverse Cuthill-McKee procedure

1976 GPS

2001 Tabu search based algorithms

A complete and detailed explanation of the algorithms is not presented here and the result of an assessment can be found in (Marti et al., 2001). Despite the reverse Cuthill-McKee procedure is not the best of the methods listed, its full implementation in MATLAB makes it inmediately available.

Appendix B

Intrinsic Apoptosis Pathway Model

```
Bir12 =
Casp3*XIAPCasp9*k18+Casp3*XIAPp2frag*k20-
Bir12*Smac*k43+Bir12Smac*k44-Bir12*k63;

Bir12Casp3 =
Bir12*Casp3*k15-Bir12Casp3*k16+Casp3*XIAPCasp3*k19+
Casp3*XIAPp2fragCasp3*k21+Casp3*XIAPCasp9Casp3*k22-
Bir12Casp3*Smac*k47+Bir12Smac*Casp3*k48-Bir12Casp3*k67;

Bir12Smac =
Casp3*XIAP2Smac*k23+Bir12*Smac*k43-Bir12Smac*k44+
Bir12Casp3*Smac*k47-Bir12Smac*Casp3*k48-Bir12Smac*k65;

Bir3R =
Casp3*XIAP*k17+Casp3*XIAPCasp3*k19-Bir3R*Casp9*k31+
Bir3RCasp9*k32+Bir3Rp2frag*k33-Bir3R*Smac*k45+
Bir3RSmac*k46-Bir3R*k64;

Bir3RCasp9 =
Casp3*XIAPCasp9*k18+Casp3*XIAPCasp9Casp3*k22-
Bir3RCasp9*Casp3*k26+Bir3R*Casp9*k31-Bir3RCasp9*k32-
Bir3RCasp9*Smac*k49+Bir3RSmac*Casp9*k50-Bir3RCasp9*k68;

Bir3RSmac =
Casp3*XIAP2Smac*k23+Bir3R*Smac*k45-Bir3RSmac*k46+
Bir3RCasp9*Smac*k49-Bir3RSmac*Casp9*k50-Bir3RSmac*k66;

Bir3Rp2frag =
Casp3*XIAPp2frag*k20+Casp3*XIAPp2fragCasp3*k21+
Bir3RCasp9*Casp3*k26-Bir3Rp2frag*k33-Bir3Rp2frag*k69;

Casp3 =
Casp9*Procasp3*k5+Casp9P*Procasp3*k7+Casp3*Procasp3*k8-
Casp3*XIAP*k9+XIAPCasp3*k10-Casp3*XIAPCasp9*k11+
XIAPCasp9Casp3*k12-Casp3*XIAPp2frag*k13+XIAPp2fragCasp3*k14-
```

```
Bir12*Casp3*k15+Bir12Casp3*k16+Smacˆ2*XIAPCasp3*k39-
Casp3*XIAP2Smac*k40+Smacˆ2*XIAPCasp9Casp3*k41-
Casp3*Casp9P*XIAP2Smac*k42+Bir12Casp3*Smac*k47-
Bir12Smac*Casp3*k48-Casp3*k55;

Casp9 =
-Casp3*Casp9*k6-Casp9*XIAP*k27+XIAPCasp9*k28-
Casp9*XIAPCasp3*k29+XIAPCasp9Casp3*k30-Bir3R*Casp9*k31+
Bir3RCasp9*k32+Smacˆ2*XIAPCasp9*k37-Casp9*XIAP2Smac*k38+
Bir3RCasp9*Smac*k49-Bir3RSmac*Casp9*k50-Casp9*k54+u1;

Casp9P =
Casp3*Casp9*k6+Casp3*XIAPCasp9Casp3*k24+
Casp3*XIAPCasp9*k25+Bir3RCasp9*Casp3*k26+
Smacˆ2*XIAPCasp9Casp3*k41-Casp3*Casp9P*XIAP2Smac*k42-
Casp9P*k53;

Procasp3 =
-Procasp3*k1+k2-Casp9*Procasp3*k5-Casp9P*Procasp3*k7-
Casp3*Procasp3*k8;

Smac =
-2*Smacˆ2*XIAP*k35+2*XIAP2Smac*k36-2*Smacˆ2*XIAPCasp9*k37
+2*Casp9*XIAP2Smac*k38-2*Smacˆ2*XIAPCasp3*k39+2*Casp3*XIAP2Smac*k40
-2*Smacˆ2*XIAPCasp9Casp3*k41+2*Casp3*Casp9P*XIAP2Smac*k42
-Bir12*Smac*k43+Bir12Smac*k44-Bir3R*Smac*k45+Bir3RSmac*k46
-Bir12Casp3*Smac*k47+Bir12Smac*Casp3*k48-Bir3RCasp9*Smac*k49
+Bir3RSmac*Casp9*k50-2*Smacˆ2*XIAPp2frag*k51
+2*XIAPp2frag2Smac*k52-Smac*k70+u2;

XIAP =
-XIAP*k3+k4-Casp3*XIAP*k9+XIAPCasp3*k10-Casp3*XIAP*k17-
Casp9*XIAP*k27+XIAPCasp9*k28+XIAPp2frag*k34-
Smacˆ2*XIAP*k35+XIAP2Smac*k36;

XIAP2Smac =
-Casp3*XIAP2Smac*k23+Smacˆ2*XIAP*k35-XIAP2Smac*k36+
Smacˆ2*XIAPCasp9*k37-Casp9*XIAP2Smac*k38+
Smacˆ2*XIAPCasp3*k39-Casp3*XIAP2Smac*k40+
Smacˆ2*XIAPCasp9Casp3*k41-Casp3*Casp9P*XIAP2Smac*k42-XIAP2Smac*k62;

XIAPCasp3 =
Casp3*XIAP*k9-XIAPCasp3*k10-Casp3*XIAPCasp3*k19-Casp9*XIAPCasp3*k29+
XIAPCasp9Casp3*k30-Smacˆ2*XIAPCasp3*k39+Casp3*XIAP2Smac*k40-XIAPCasp3*k56;

XIAPCasp9 =
-Casp3*XIAPCasp9*k11+XIAPCasp9Casp3*k12-Casp3*XIAPCasp9*k18-
Casp3*XIAPCasp9*k25+Casp9*XIAP*k27-XIAPCasp9*k28-
Smacˆ2*XIAPCasp9*k37+Casp9*XIAP2Smac*k38-XIAPCasp9*k58;

XIAPCasp9Casp3 =
Casp3*XIAPCasp9*k11-XIAPCasp9Casp3*k12-Casp3*XIAPCasp9Casp3*k22-
Casp3*XIAPCasp9Casp3*k24+Casp9*XIAPCasp3*k29-XIAPCasp9Casp3*k30-
Smacˆ2*XIAPCasp9Casp3*k41+Casp3*Casp9P*XIAP2Smac*k42-XIAPCasp9Casp3*k57;

XIAPp2frag =
-Casp3*XIAPp2frag*k13+XIAPp2fragCasp3*k14-Casp3*XIAPp2frag*k20+
```

```
Casp3*XIAPCasp9*k25-XIAPp2frag*k34-Smacˆ2*XIAPp2frag*k51+
XIAPp2frag2Smac*k52-XIAPp2frag*k59;

XIAPp2frag2Smac =
Smacˆ2*XIAPp2frag*k51-XIAPp2frag2Smac*k52-XIAPp2frag2Smac*k61;

XIAPp2fragCasp3 =
Casp3*XIAPp2frag*k13-XIAPp2fragCasp3*k14-
Casp3*XIAPp2fragCasp3*k21+Casp3*XIAPCasp9Casp3*k24-
XIAPp2fragCasp3*k60]
```

Appendix C

PD controller in the INAP

This Appendix shows the proof of (3.5) in Section 3.2.1.

Claim C.1. *The regulators of $\mathcal{P}_1$ and $\mathcal{P}_2$ (Section 3.2.1)are proportional derivative controllers.*

Proof. The main plot of the proof is algebraic substitution in the differential equation corresponding to Caspase 3 and 9. This is motivated by the biological fact the inhibitor of caspases acts over the activated version of the casapases. That is to say control signal will be present in the differential equation of the activated version of the both Caspase 3 and 9.
Caspase 9 The variation in the concentration of Caspase 9 is:

$$\begin{aligned}[\dot{C_{9a}}] &= -\left(k_6[C_{3a}] + k_{29}[XIAPC_{3a}] + k_{54}\right)[C_{9a}] + \\ &\quad + u_{R_1-P_2} + u_{R_3-P_2} + u_1 \end{aligned} \tag{C.1}$$

where

$$\begin{aligned} u_{R_1-P_2} &\equiv -\left(k_{31}Bir3R + k_{50}[Bir3RSmac]\right)[C_{9a}] + \\ &\quad + k_{32}[Bir3RC_{9a}] + k_{49}[Bir3RC_{9a}][Smac] \\ u_{R_3-P_2} &\equiv -\left(k_{27}[XIAP] + k_{38}[XIAP2Smac]\right)[C_{9a}] + \\ &\quad + k_{28}[XIAPC_{9a}] + k_{37}[Smac]^2[XIAPC_{9a}] \\ u_{R_3b-P_2} &\equiv (k_{11} - k_{22})[C_{3a}][XIAPC_{9a}] - k_{12}[XIAPC_{9a}C_{3a}] \\ u_{P_1-P_1} &\equiv -[C_{3a}]\left(k_{24}[XIAPC_{9a}C_{3a}] + k_{25}[XIAPC_{9a}] + k_{26}[Bir3RC_{9a}]\right) - \\ &\quad - k_{41}[Smac]^2[XIAPC_{9a}C_{3a}] + k_{42}[C_{3a}][C_{9a}][XIAP2Smac] \end{aligned}$$

from the interconnection of systems (see Figure 3.9):

$$\begin{aligned}
u_{R_1-P_2} &= -\mathcal{P}\partial\mathcal{K}_{k_{68}}^{k_{26}}\{[Bir3RC_{9a}]\} + \\
&\quad +[C_{3a}]\left(k_{18}[XIAPC_{9a}] + k_{22}[XIAPC_{9a}C_{3a}]\right) \\
u_{R_3-P_2} &= -\mathcal{P}\partial\mathcal{K}_{k_{58}}^{k_{25}}\{[XIAPC_{9a}]\} - \\
&\quad -[C_{3a}]\left((k_{18}+k_{11})[XIAPC_{9a}] + k_{12}[XIAPC_{9a}C_{3a}]\right) \\
u_{R_{3b}-P_2} &= -\mathcal{P}\partial\mathcal{K}_{k_{57,30}}^{k_{24}}\{[XIAPC_{9a}C_{3a}]\} + \\
&\quad +k_{29}[C_{9a}][XIAPC_{3a}] - \\
&\quad -k_{41}[XIAPC_{9a}C_{3a}][Smac]^2 + k_{42}[C_{3a}][C_{9a}][XIAP2Smac] \\
u_{P_1-P_1} &= -\mathcal{P}\partial_{k_{53}}\{[C_{9P}]\} + k_6[C_{3a}][C_{9a}]
\end{aligned} \tag{C.2}$$

where

$$\begin{aligned}
\mathcal{P}\partial\mathcal{K}_{k_a}^{k_b}\{\gamma\} &= \mathcal{P}\partial_{k_a}\{\gamma\} + k_b[C_{3a}]\gamma \\
\mathcal{P}\partial_{k_a}\{\gamma\} &= \dot{\gamma} + k_a\gamma
\end{aligned} \tag{C.3}$$

Substituting the last four equations in (C.1),

$$\begin{aligned}
\dot{[C_{9a}]} &= -k_{54}[C_{9a}] - \mathcal{P}\partial_{k_{53}}\{[C_{9P}]\} - \mathcal{P}\partial_{k_{58}}\{[XIAPC_{9a}]\} - \\
&\quad -\mathcal{P}\partial_{k_{57,30}}\{[XIAPC_{9a}C_{3a}]\} - \mathcal{P}\partial_{k_{68}}\{[Bir3RC_{9a}]\} + \\
&\quad +u_1
\end{aligned} \tag{C.4}$$

Caspase 3
For the activated version of Caspase 3:

$$\begin{aligned}
\dot{[C_{3a}]} &= \left(k_5[C_{9a}] + k_7[C_{9P}] + k_8[C_{3a}]\right)[C_3] - k_{55}[C_{3a}] + \\
&\quad +k_{41}[XIAPC_{9a}C_{3a}][Smac]^2 - k_{42}[C_{3a}][C_{9a}][XIAP2Smac] \\
&\quad +u_{R_2-P_2} + u_{R_4-P_2} + u_{R_{2b}-P_2} + u_{R_{3b}-P_2}
\end{aligned} \tag{C.5}$$

where

$$\begin{aligned}
u_{R_2-P_2} &\equiv -\left(k_{15}[Bir12] + k_{48}[Bir12Smac]\right)[C_{3a}] + \\
&\quad +\left(k_{16} + k_{47}[Smac]\right)[Bir12C_{3a}] \\
u_{R_4-P_2} &\equiv -\left(k_9[XIAP] + k_{40}[XIAP2Smac]\right)[C_{3a}] + \\
&\quad +\left(k_{10} + k_{39}[Smac]^2\right)[XIAPC_{3a}] \\
u_{R_{2b}-P_2} &\equiv -k_{13}[XIAPp2fragC_{3a}] + k_{14}[XIAPp2fragC_{3a}] \\
u_{R_{3b}-P_2} &\equiv -k_{11}[XIAPC_{9a}][C_{3a}] + k_{12}[XIAPC_{9a}C_{3a}]
\end{aligned}$$

from the other systems

$$
\begin{aligned}
u_{R_2-P_2} &= -\mathcal{P}\partial_{k_{67}}\{[Bir12C_{3a}]\} + [C_{3a}]\,(k_{19}[XIAPC_{3a}] \\
&\quad +k_{21}[XIAPp2fragC_{3a}] + k_{22}[XIAPC_{9a}C_{3a}]) \\
u_{R_4-P_2} &= -\mathcal{P}\partial\mathcal{K}^{k_{19}}_{k_{56}}\{[XIAPC_{3a}]\} - k_{29}[C_{9a}][XIAPC_{3a}] + \\
&\quad +k_{30}[XIAPC_{9a}C_{3a}] \\
u_{R_{2b}-P_2} &= -\mathcal{P}\partial\mathcal{K}^{k_{21}}_{k_{60}}\{[XIAPp2fragC_{3a}]\} + k_{24}[C_{3a}][XIAPC_{9a}C_{3a}] \\
u_{R_{3b}-P_2} &= -\mathcal{P}\partial_{k_{57}}\{[XIAPC_{9a}C_{3a}]\} - (k_{22}+k_{24})[C_{3a}][XIAPC_{9a}C_{3a}] + \\
&\quad +k_{29}[C_{9a}][XIAPC_{3a}] - k_{30}[XIAPC_{9a}C_{3a}] + \\
&\quad +k_{42}[C_{3a}][C_{9a}][XIAP2Smac] - k_{41}[XIAPC_{9a}C_{3a}][Smac]^2
\end{aligned}
$$

substituting the last four equations in (C.5),

$$
\begin{aligned}
\dot{[C_{3a}]} &= (k_5[C_{9a}] + k_7[C_{9P}] + k_8[C_{3a}])\,[C_3] - k_{55}[C_{3a}] \\
&\quad -\mathcal{P}\partial_{k_{56}}\{[XIAPC_{3a}]\} - \mathcal{P}\partial_{k_{57}}\{[XIAPC_{9a}C_{3a}]\} \\
&\quad -\mathcal{P}\partial_{k_{60}}\{[XIAPp2fragC_{3a}]\} - \mathcal{P}\partial_{k_{67}}\{[Bir12C_{3a}]\} \qquad \text{(C.6)}
\end{aligned}
$$

□

Note that in (C.4 and C.6) four different PD controllers are present,i.e., there are *four mechanisms* to regulate each one of the activated versions of the caspases involved.

Appendix D

SSV code

This section contains the scripts used in the present work.

D.1 Model linearization

file ./Eissing04/Robust/LinearizeModel.m

```
%This function construct the Jacobian
%of Eissings04 model with different
%options: symbolical, evaluating
%parameters to zero, numerical
%substitution, and others.

%'a' is the variable which
%is to be preserved in the bock.
%if no input is %applied then
%every parameter is
%to be preserved.

%Input b stands for the steady state
%to evaluate the Jacobian

%if c = 'numeric' then parameters are
%evaluated in the nominal value

function A = LinearizeModel(a,b,c)

%Detecting if there has been an input
%to the function
if nargin == 0
    a = 0;
    b = 0;
    c = 0;
elseif nargin == 1
    b = 0;
    c = 0;
elseif nargin == 2
    c = 0;
```

```
end

if iscell(a)
    q = 'y';
else
    q = 'n';
    if a ~= 0
        a = {a};
        q = 'y';
    end
end

na = size(a);
na = na (1,2);


%Parameters definition
syms k1 k2 k3 k4 k5 k6 k7 k8 k9
k10 k11 k12 k13 km3 km8 km9 km10 km11 km12
p = [k1 k2 k3 k4 k5 k6 k7 k8 k9
k10 k11 k12 k13 km3 km8 km9 km10 km11 km12];
np = size(p);
np = np(1,2);
pn = [5.8e-05 1.0e-05 0.0005 0.0003 0.0058
0.0058 0.0173 0.0116 0.0039 0.0039
0.0005 0.001 0.0116 0.21 464 507 81.9 0.21 40];
dimension = 8; %Dimension of the state space

%States definition
syms c8 c8a c3 c3a IAP c3aIAP CARP c8aCARP
x = [c8 c8a c3 c3a IAP c3aIAP CARP c8aCARP];

%Reactions definitions
v1 = k1*c8a*c3;
v2 = k2*c3a*c8;
v3 = k3*c3a*IAP-km3*c3aIAP;
v4 = k4*c3a*IAP;
v5 = k5*c8a;
v6 = k6*c3a;
v7 = k7*c3aIAP;
v8 = k8*IAP - km8;
v9 = k9*c8-km9;
v10 = k10*c3-km10;
v11 = k11*c8a*CARP-km11*c8aCARP;
v12 = k12*CARP-km12;
v13 = k13*c8aCARP;

%Differential states system
c8p = -v2-v9;
c8ap = v2-v5-v11;
c3p = -v1-v10;
c3ap = v1-v3-v6;
IAPp = -v3-v4-v8;
c3aIAPp = v3-v7;
CARPp = -v11-v12;
c8aCARPp = v11-v13;
```

```
%Computing Jacobian
A = Jacobian([c8p c8ap c3p c3ap IAPp c3aIAPp CARPp c8aCARPp],
[c8 c8a c3 c3a IAP c3aIAP CARP c8aCARP]);

switch q
    case 'n'
        fprintf('   No parameter set to zero.\n')
    case 'y'
        %Find which index of the parameter vector are to be kept
        k = 1;
        q = 0;
        if na > 1
            for j = 1:na
                for i =1:np
                    d = sym(cell2mat(a(1,j)));
                    if d == p(1,i)
                        keep(k) = i;
                        k = k+1;
                    end
                end
            end
        elseif na == 1
                for i =1:np
                    d = sym(cell2mat(a));
                    if d == p(1,i)
                        keep(k) = i;
                    end
                end
        end

        try
            keep;
        catch
            q = 1;
        end

        switch q
            case 0
                k = 1;
                i = 1;
                %Loop that sets the unwanted parameters to zero
                while (i <= np)
                    if i == keep(1,k)
                        fprintf('Do not errase. %i\n',i)
                        if k < na
                            k = k+1;
                        end
                    else
                        %fprintf('Errase. %i\n',i)
                        A = subs(A,p(1,i),0);
                    end
                    i = i +1;
                end
            case 1
                fprintf('No such parameter.\n')
        end
end
```

```
%Evaluate the parameters and the states in the
%nominal value in order to have a numeric matrix
if size(b) == [1 dimension]
    for i = 1:dimension
       A = subs(A,x(1,i),b(1,i));
    end
    fprintf('      Evaluating the Jacobian in the
requested state.\n')
    A = vpa(A,3);
else
    fprintf('      Neither state nor parameter evaluation.\n')
end

%Evaluate the parameters in the nominal value.
if c == 'numeric'
          fprintf('         Evaluating the parameters in
the nominal value.\n')
          for i = 1:np
              A = subs(A,p(1,i),pn(1,i));
          end
          A = A;
end
```

D.2 Computing the SSV

file ./Eissing04/Robust/MuiII.m Function call: (MuiII(sys.a,FP))

```
function Miu = Main(A,FP)
clc
close all

for i = 1:19
    try
        Miu(i,:) = body(A,FP,i);
    catch
        fprintf('            Error in Body.@ %i\n',i)
        %Mui(i,:) = [0,0];
    end
end
clc

function m = body(A,FP,i)
syms p k
tol = 0.98;
q = {'k1' 'k2' 'k3' 'k4' 'k5' 'k6' 'k7' 'k8' 'k9'
'k10' 'k11' 'k12' 'k13' 'km3' 'km8' 'km9' 'km10' 'km11' 'km12'};
pn = [5.8e-05 1.0e-05 0.0005 0.0003 0.0058 0.0058
0.0173 0.0116 0.0039 0.0039 0.0005 0.001 0.0116 0.21 464 507 81.9 0.21 40];

G = inv(p*eye*(8)-A);
Delta = subs(LinearizeModel(q(1,i),FP(1,:)),q(1,i),pn(1,i));

MDelta = k*G*Delta;

[num den] = numden(solve(det(eye(8) - MDelta),k));
num = sym2poly(num);
```

```
den = sym2poly(den);
[mag phase omega] = bode(tf(num,den),{1e-20 100000});
[k j] = min(mag);

%Corrects the sign of the perturrbation
if and(phase(j) < 360, phase(j) > 180)
    k = k;
else
    k = -k;
end

% %%%Miu plot
% figure('Name', strcat('Parameter_',
int2str(i), ' RS')  ,'Position',[0 500 1050 500]);
% bodemag(tf(k*den,num));
% grid;

%%% Robust Performance
syms y
We = 50000*(0.1*p + 0.001)/(p + 0.0001);
C = [0 0 0 1 0 0 0 0];
B = [0 1 0 0 0 0 0 0]';
fprintf('                            Now computing the
 maximal allowed pertubation in order
to maintain a performance index...\n')
%Norm of the perturbation
Beta = vpa(1/(y*norm(Delta,inf)),1);

%Transfer function from u(initial condition of C8a) to z (weighted error)
Cl = simplify(We * C * G * y * Delta*inv(eye(8) - G* y * Delta) * G * B);
[num den] = numden(1/Beta * Cl);

% Search for a convex property algorithm
LB = 0.000000005;
pitch = 3;
UB = LB + pitch;
Me = (LB + UB) / 2;

while pitch > 0.000000001
    PropLB = maximal(num, den, LB);
    PropUB = maximal(num, den, UB);

    if and(PropLB < tol, PropUB > tol)
        pitch = 0.1 * pitch;
        LB = Me - pitch;
        UB = Me + pitch;
        Mean = (LB + UB) / 2;
    elseif and(PropUB < tol, PropLB < tol)
        LB = UB;
        UB = UB + pitch;
        Me = (LB + UB) / 2;
    elseif and(PropLB > tol, PropUB > tol)
        LB = LB  - pitch;
        UB = LB;
        Me = (LB + UB) / 2;
    end
end
```

```
%%% Mui Plot for robust performance
% num = sym2poly(subs(num,'y',Me));
% den = sym2poly(subs(den,'y',Me));
% figure('Name', strcat('Parameter_',  int2str(i), ' RP'),
'Position',[0 500 1050 500]);
% bodemag(tf(num, den));
% grid

m=[k 100*k/pn(1,i) Me 100*Me/(pn(1,i))]

%Computes the singular structured singular value
function r = maximal(num,den,j)
syms y
num = sym2poly(subs(num,'y',j));
den = sym2poly(subs(den,'y',j));
[mag phase omega] = bode(tf(num,den));
r = max(mag);
```

D.3 Variation of parameters to determine the stability bounds

file ./Eissing04/Robust/DeltaII.m function call: DeltaII(FP)

```
%This function determine the maximal variation
%in a parameter while preserving stability in
%the pertrubing system.

%Regarding the perturbed model, it varies one
%parameter perturbation  at a  time in order to
%compute the eigenvalues and determine the stability.

%The algoritm which searches the maximum allowed
%perturbation is incremental (SLOW!)

%This values can be used to determine bounds.

function Bound = DeltaII(SS)
for j = 1:19
    Bound(1,j) = Ciclic(SS,j,1);
    Bound(2,j) = Ciclic(SS,j,0);
end

function bound = Ciclic(SS,j,sign)

%Parameter definition and nominal values
p = {'k1' 'k2' 'k3' 'k4' 'k5' 'k6' 'k7' 'k8'
'k9' 'k10' 'k11' 'k12' 'k13' 'km3'
'km8' 'km9' 'km10' 'km11' 'km12'};
pn = [5.8e-05 1.0e-05 0.0005 0.0003 0.0058
0.0058 0.0173 0.0116 0.0039 0.0039
0.0005 0.001 0.0116 0.21 464 507
81.9 0.21 40];
delta = 0;
i = 0;
if sign == 0
```

```
    sign = -1;
end

A = LinearizeModel(0,SS,'numeric');
stable = isstable(A);
clc

%Delta matrix of perturbation
Cosa = subs(LinearizeModel(p(1,j),SS),p(1,j),pn(1,j));
pitch = sign * pn(1,j) / 100;

[U S V] = svd (Cosa,'econ');
U = U(:,1);
S = S(1,1);
V = V(:,1);

W1 = U;
W2 = S*V';

%Perturbing the original system
Cl = A + U*delta*S*V';

fprintf('Determining largest
allowable perturbation
before instability.\n');
if S ~= 0
    while stable == 1
           i = i + 1;
        delta = delta + pitch;
        Cl = A + W1*delta*W2;
        stable = isstable(Cl);
        if i > 1000000
            stable = 0;
            delta = 0;
        end
    end
else
    delta = 0;
end

bound = pn(1,j) + delta;

function stable = isstable(A)
%Parameter definition
stable = 1;

r = eig(A);
t = size(r);
t = t(1,1);

for i=1:t
    if r(i,1) > 0 %Positive EigenValue!
        eig(A)
        stable = 0;
    end
end
```

Bibliography

Alberts, B., A. Johnson, J. Lewis, M. Raff, K. Roberts, and P. Walter (2002). *Molecular Biology of the Cell, Fourth Edition*. Garland.

Alvarez, J. (2008). Control de procesos químicos. Lecture, UNAM.

Angeli, D., J. Ferrel, and E. Sontag (2004, Feb.). Detection of multistability, bifurcations and hysteresis in a large vlass o biological positive-feedback systems. *PNAS*.

Angeli, D. and E. Sontag (2003a, Oct.). Monotone control systems. *Automatic Control, IEEE Transactions on 48*(10), 1684–1698.

Angeli, D. and E. Sontag (2003b). Multi-stability in monotone input/output systems. *Systems & Control Letters*.

Bullinger, E. (2005, Dec.). System analysis of a programmed cell death model. In *Decision and Control, 2005 and 2005 European Control Conference. CDC-ECC '05. 44th IEEE Conference on*, pp. 7994–7999.

Carotenuto, L., V. Pace, D. Bellizzi, and D. B. G. (2007). Equilibrium, stability and dynamical response in a model of the extrinsic apoptosis pathway. *Journal of Biologial Systems*.

Cuthill, E. and J. McKee (1969). Reducing the bandwidth of sparse symmetric matrices. In *Proceedings of the 24th National Conference*, New York, NY, USA, pp. 157–172. ACM.

Diestel, R. (2000). *Graph Theory*. Springer-Verlag.

Dunne, R. (2008). Intership report. Hamilton Institute NUIM.

Eissing, T. (2007). *A Systems Science View on Cell Death Signalling*. Ph. D. thesis, Universität Stuttgart.

Feinberg, M. (1979). Lectures on chemical reaction networks.

Hirsch, J. and H. Smith (2005). Monotone dynamical systems. in Handbook of Differential Equations, Ordinary Differential Equations.

Khalil, H. K. (2001, December). *Nonlinear Systems (3rd Edition)*. Prentice Hall.

Kitano, H. (2001). *Foundations of Systems Biology*. The MIT Press.

Klipp, E., A. Kowald, C. Wierling, and H. Lehrach (2005, May). *Systems Biology in Practice: Concepts, Implementation and Application*. Wiley-VCH.

Lockshin, R. and Z. Zakeri (2004). Apoptosis, autophagy and more. *IJBCB*.

Marti, R., M. Laguna, F. Glover, and V. Campos (2001, December). Reducing the bandwidth of a sparse matrix with tabu search. *European Journal of Operational Research 135*(2), 450–459.

Otero-Muras, I., J. Banga, and A. Alonso (2009). Theoretical basis for detecting bifurcations in biochemical reaction networks. *To appear*.

Paul, P., D. Kalamatianos, H. Duessmann, and H. Huber (2008). Automatic quality assessment for fluorescence microscopy images. *8th IEEE International Conference on BioInformatics and BioEngineering*.

Rai, N., K. Tripathi, D. Sharma, and V. Shukla (2005). Apoptosis: a basic physiologic process in wound healing. *Sage Publications*.

Rehm, M., H. Huber, H. Dussmann, and J. Prehn (2006, August). Systems analysis of effector caspase activation and its control by x-linked inhibitor of apoptosis protein. *EMBO*.

Schrödinger, E. (1944). *What is life? and other scientific essays*. Doubleday, Garden City, N.Y.

Shoemaker, J. and F. r. Doyle (2008). Identifying fragilities in biochemical networks: Robust performance analysis of fas signaling-induced apoptosis. *Biophysical Journal*.

Skogestad, S. and I. Postlethwaite (1996). *Multivariable Feedback Control: Analysis and Design*. John Wiley & Sons.

Sontag, E. (2005, Dec.). Molecular systems biology and control: A qualitative-quantitative approach. pp. 2314–2319.

Watson, J. and F. Crick (1953). Molecular structure of nucleic acids. *Nature*.

Wellstead, P., E. Bullinger, D. Kalamatianos, O. Mason, and M. Verwoerd (2008). The role of control and systems theory in systems biology. *Annual Reviews in Control*.

Wurzer, W. J., O. Planz, C. Ehrhardt, M. Giner, T. Silberzahn, S. Pleschka, and S. Ludwig (2003, June). Caspase 3 activation is essential for efficient influenza virus propagation. *The EMBO journal 22*(11), 2717–2728.

Zhou, K., J. C. Doyle, and K. Glover (1996). *Robust and Optimal Control*. Prentice Hall.

Index